

JAERI-Research

JP0050355

2000-012



FRACTURE MECHANICS ANALYSIS AND EVALUATION FOR THE RPV OF
THE CHINESE QINSHAN 300MW NPP UNDER PTS

March 2000

Yinbiao HE* and Toshikuni ISOZAKI

日本原子力研究所
Japan Atomic Energy Research Institute

本レポートは、日本原子力研究所が不定期に公刊している研究報告書です。
入手の問合せは、日本原子力研究所研究情報部研究情報課（〒319-1195 茨城県那
珂郡東海村）あて、お申し越し下さい。なお、このほかに財団法人原子力弘済会資料セ
ンター（〒319-1195 茨城県那珂郡東海村日本原子力研究所内）で複写による実費頒布
を行っております。

This report is issued irregularly.

Inquiries about availability of the reports should be addressed to Research
Information Division, Department of Intellectual Resources, Japan Atomic Energy
Research Institute, Tokai-mura, Naka-gun, Ibaraki-ken 〒319-1195, Japan.

Fracture Mechanics Analysis and Evaluation for the RPV of the Chinese Qinshan 300MW NPP under PTS

Yinbiao HE * and Toshikuni ISOZAKI

Department of Reactor Safety Research
Nuclear Safety Research Center
Tokai Research Establishment
Japan Atomic Energy Research Institute
Tokai-mura, Naka-gun, Ibaraki-ken

(Received January 31, 2000)

One of the most severe accident conditions of a reactor pressure vessel (RPV) in service is the loss of coolant accident (LOCA). Cold safety injection water is pumped into the downcomer of the RPV through inlet nozzles, while the internal pressure may remain at high level. Such an accident is called pressurized thermal shock (PTS) transient according to 10 CFR 50.61 definition. This paper illustrates the fracture mechanics analysis for the existing RPV of the Chinese Qinshan 300MW nuclear power plant (NPP) under the postulated PTS transients that include SB-LOCA, LB-LOCA of Qinshan NPP and Rancho Seco transients. 3-D models with the flaw depth range $a/w=0.05\sim 0.9$ (a : flaw depth; w : wall thickness) were used to probe what kind of flaw and what kind of transient are most dangerous for the RPV in the end of life (EOF). Both the elastic and elastic-plastic material models were used in the stress analysis and fracture mechanics analysis. The different types of flaw and the influence of the stainless steel cladding on the fracture analysis were investigated for different PTS transients. Comparing with the material initiation crack toughness K_{IC} , the fracture evaluation for the RPV in question under PTS transients are performed in this paper.

Keywords: RPV, Core Beltline, PTS, Shallow and Deep Flaws, Fracture Mechanics

* on leave from Shanghai Nuclear Engineering Research and Design Institute

中国秦山 300MW 原子力プラント圧力容器における
加圧下熱衝撃時の破壊力学解析

日本原子力研究所東海研究所安全性試験研究センター原子炉安全工学部

賀 寅彪*・磯崎 敏邦

(2000 年 1 月 31 日受理)

原子炉圧力容器の想定重大事故のひとつに冷却材喪失(LOCA)があり、その際には、内圧が高い状態でノズルからダウンカマーへと冷却水が注入され、加圧下熱衝撃(PTS)が生じる。

本報は、中国秦山 300MW 原子力プラント圧力容器に対して想定される小規模 LOCA, 大規模 LOCA の際の加圧下熱衝撃時の破壊力学解析結果をまとめたものである。圧力容器の寿命に対する欠陥の種類や圧力変動の違いの影響を探るために3次元モデルを用い、また、応力および破壊力学解析には弾性および弾塑性モデルを用いた。異なるタイプの欠陥およびステンレス肉盛り溶接部の影響を種々の PTS 変動について調べ、破壊靭性値 K_{IC} と比較することにより、PTS 時の破壊評価を行った。

Contents

1.	Introduction	1
2.	Structural Model and Assumptions for the Analysis	2
3.	Material Properties and Loading Conditions	3
4.	Method of Fracture Mechanics Analysis	4
5.	Results	5
5.1	Verification for the Model and the Method (No Thermal Shock).....	5
5.2	The Results from Qinshan SB-LOCA and Rancho Seco	6
5.3	The Results from LB-LOCA	7
5.4	Surface Flaw and Sub-surface Flaw	7
5.5	Influence of Cladding	8
6.	Conclusion	9
	Acknowledgment.....	9
	References	10
	Appendix	22

目 次

1.	はじめに	1
2.	解析用の構造モデルと仮定	2
3.	材料特性と荷重条件	3
4.	破壊力学解析手法	4
5.	結果	5
5.1	モデルと手法の検証（熱衝撃なし）	5
5.2	秦山の小破断 LOCA とランチョオセコの結果	6
5.3	大破断 LOCA の結果	7
5.4	表面き裂と埋没き裂	7
5.5	クラッドの影響	8
6.	まとめ	9
	謝辞	9
	参考文献	10
	付録	22

This is a blank page.

1. Introduction

The reactor pressure vessel (RPV) integrity is ensured by a margin between its load bearing capacity (material properties) and the applying loads during operation. Structural integrity research for RPV is a large-scale research project including the thermal hydraulic analysis concerning selecting transients, the structural analysis concerning fracture mechanics assessment and the material properties concerning embrittlement, annealing behavior. For the RPV integrity it is not adequate to fulfill the fracture evaluation in accordance with App. G of ASME B&PV code III[1] and the additional works should be taken into account after the plant got the operating license. Such works should meet the requirements of 10 CFR 50.61[2], R.G 1.154[3] and R.G 1.99[4] to ensure the RPV integrity under the pressurized thermal shock (PTS), which would occur during the postulated loss of coolant accident (LOCA). It is mentioned in 10 CFR 50.61 that for each pressurized water nuclear power reactor, the value of RT_{PTS} for any material in beltline is projected to exceed the PTS screening criterion using EOF (end of life) fluence. The licensee must submit a safety analysis at least three years before RT_{PTS} , RT_{NDT} for EOF fluence, exceeds the PTS screening criterion. It means the plant cannot continue to operate without justification when RT_{PTS} is beyond PTS screening criterion.

The objective of the research described in this paper was to perform the fracture mechanics analysis for the existing RPV of Qinshan NPP under the postulated PTS transients. Such an analysis is both a part of PTS analysis report, which shall be submitted when the RT_{PTS} is anticipated to exceed the PTS screening criterion, and an assessment method for the flaw, which might be detected during inservice inspection in accordance with ASME B&PV code XI[5].

The different flaw sizes, different types of flaw and different PTS transients were considered and compared to determine what kind of flaw and what kind of transient are most dangerous for the RPV. During the analysis two material models were applied to the stress calculations of the RPV. One is the thermal-elastic material model and the other is thermal-elastic-plastic material model. The analysis accounted for the influence of the stainless steel cladding on the fracture analysis. The fracture mechanics analysis was performed by the internationally used ADINA code [6]. The virtual crack extension (VCE) method [7] was employed to obtain the fracture mechanics parameter J-integral, and then converted to the stress intensity factor K_J for the comparison

with the material fracture toughness. The analytical calculation [8-9] and ASME code method [1] for K_I had been taken into account to verify the reliability of the models and the computation method and the applicability of ADINA code. The comparison shows that the result from FEM has a good agreement with the results from the other two methods.

The fracture mechanics analysis and evaluation for the RPV in question are set forth by a flow chart, which is shown in Fig.1.

2. Structural model and assumptions for the analysis

The RPV of Qinshan 300MW NPP was designated to bear high temperature, high pressure and corrosion of the primary system coolant and the neutron irradiation for the core beltline during the license lifetime. The weld is sensitive to the irradiation embrittlement caused by the relatively high neutron flux on the vessel wall. The core beltline was manufactured by the SA-508 class 3 ring forging to avoid the axial welding seam and connected to nozzle belt and bottom head with two circumferential welding seams. Comparing with other parts of the RPV, the core beltline suffers the strongest neutron irradiation leading to a significant nil-ductility transition temperature increment and embrittlement in EOF. So the core beltline was taken as a model for the fracture mechanics analysis. The main design parameters and dimensions are as follows:

Main design parameters:

Design pressure	17.2MPa
Normal operating pressure	15.2MPa
Hydrostatic test pressure	21.5MPa
Design temperature	350°C
Normal operating inlet temperature	288.8°C
Normal operating outlet temperature	315.2°C
Hydrostatic test temperature	33°C (shop test) /60°C (site test)
Design life	30 years

Main dimensions for core beltline:

Inner diameter of core beltline	3374mm
Wall thickness of core beltline	174mm (including the cladding)
Thickness of cladding	4mm

An axial inner surface flaw or sub-surface flaw is assumed to exist in the beltline before the PTS transient occurs. Several models with different flaw sizes ($a/w=0.05\sim0.9$) were created using ADINA-IN in order to investigate the influence of the flaw size. The parameter design technology was applied to the model creating procedure to reduce the pre-processing work of several models as possible. To eliminate the boundary effects, the model with 90 degree along circumferential direction and 1500mm height along axial direction were adopted for both the thermal analysis and the stress analysis. The discrete model was obtained with about 6400 3-D elements with middle nodes and 32000 nodes. The model and mesh are shown in Fig. 2.

The stainless steel cladding is involved in these models. For the worst condition, it was assumed that there were map cracking in the cladding before the LOCA would occur. It means that the cladding would be able to conduct heat flux but lose its strength to bear the loads. Omitting the couple effect, the uncoupled thermal and stress analyses were performed respectively. The discontinuity of stress at the interface between the base and cladding due to the difference in Young's modulus is taken into account.

3. Material properties and loading conditions

The core beltline was manufactured using SA-508 class.3 forging and its inner surface was welded using E308L weld metal to form a stainless steel cladding of 4mm in thickness. For the transient thermal and stress analyses, all thermal and mechanical properties of the base and cladding materials are changed with the relevant temperature and listed in the Table 1 and Table 2.

Table 1 Thermal and mechanical properties for the base material

Temperature	Conductivity	Specific heat	Young's modulus	Poisson's ratio	Mean coef. of thermal expansion
°C	W/(m × °C)	J/(m³ × °C)	GPa		1/°C
50	38.3	3.61×10^6	200	0.3	11.75×10^{-6}
100	38.8	3.79×10^6	196	0.3	12.07×10^{-6}
150	38.8	3.94×10^6	193	0.3	12.39×10^{-6}
200	38.6	4.09×10^6	189	0.3	12.69×10^{-6}
250	38.1	4.23×10^6	187	0.3	12.99×10^{-6}
300	37.5	4.4×10^6	184	0.3	13.29×10^{-6}
350	36.8	4.56×10^6	177	0.3	13.57×10^{-6}

Table 2 Thermal and mechanical properties for the cladding material

Temperature	Conductivity	Specific heat	Young's modulus	Poisson's ratio	Mean coef. of thermal expansion
°C	W/(m × °C)	J/(m³ × °C)	GPa		1/°C
50	13.9	3.94×10^6	193	0.3	15.45×10^{-6}
100	14.6	4.0×10^6	190	0.3	15.86×10^{-6}
150	15.6	4.17×10^6	186	0.3	16.26×10^{-6}
200	16.3	4.19×10^6	183	0.3	16.63×10^{-6}
250	17.2	4.3×10^6	179	0.3	16.96×10^{-6}
300	18.0	4.35×10^6	175	0.3	17.25×10^{-6}
350	18.6	4.38×10^6	172	0.3	17.52×10^{-6}

On the basis of the material tensile tests, the four stress-strain curves were used to simulate the base and the cladding elastic-plastic behavior in the room and high temperatures respectively. The curves are shown in Fig.3.

The initial reference nil ductility transition temperature was measured by Charpy impact and Drop weight tests and $RT_{NDT} = -20$ °C for beltline. The K_{IC} fracture toughness curve, which is provided in ASME B&PV code XI, was used in fracture evaluation. It is assumed that the same shape of the curve may be used for all material state and the curve is only shifted along the temperature axis corresponding to the RT_{NDT} . During service the neutron irradiation can cause damage in microstructure of materials and leads to an increase in strength and a decrease in toughness. Consequently, the K_{IC} curve will be shifted to high temperature. According to 10 CFR 50.61 and R.G 1.99 the final adjusted RT_{NDT} was estimated in the design stage, $ART_{NDT} = 70$ °C [10], but the value must be corrected based on the periodical capsule specimen tests and the actual neutron irradiation fluence. For the PTS safety analysis, the ART_{NDT} is that very RT_{PTS} defined in 10 CFR 50.61.

The full power state was regarded as the so-called initial condition for both thermal analysis and stress analysis. The SB-LOCA, LB-LOCA[11] and idealized Rancho Seco[12] PTS transients are treated as the loads for the fracture analysis and shown in Figs 4~6.

4. Method of fracture mechanics analysis

The axial semi-elliptical inner surface flaw was assumed for each model and the aspect ratio of the depth (a) to the length (2c) is 1/6. The models with

flaw depth range $a/w = 0.05 \sim 0.9$ were considered.

The effects of thermal loads and pressure loads on the faces of the crack can be included in computed J-integral. The stress intensity factor was derived from the following formula:

$$K_J = \sqrt{\frac{EJ}{1-\nu^2}}$$

The linear and nonlinear fracture mechanics analysis can be performed for the elastic and the elastic-plastic material models with ADINA.

5. Results

5.1 Verification for the model and the method (no thermal shock)

The model with the axial inner surface flaw of $a/w=0.25$ in depth subject to the normal operating internal pressure ($p=15.2$ MPa) was computed by three methods: code method, analytical method and FEM.

Code method:

According to ASME B&PV code III App. G:

$$K_{I_m} = M_m \cdot \sigma_m$$

where

$$\sigma_m = pR/t = 151.2 \text{ MPa}$$

$$M_m = 0.3984 \sqrt{m} \text{ obtained from Fig. G-2214-1 of App. G}$$

$$\text{So } K_{I_m} = 60.24 \text{ MPa} \sqrt{m}.$$

Analytical method:

According to ref. [8-9]:

$$K_I = \frac{pR}{t} \sqrt{\pi \frac{a}{Q}} F_i \left(\frac{a}{c}, \frac{a}{t}, \frac{t}{R}, \phi \right)$$

where

F_i : Boundary correction factor

$$F_i = \frac{t}{R} \left(\frac{R_0^2}{R_0^2 - R^2} \right) \left[2G_0 - 2\left(\frac{a}{R}\right)G_1 + 3\left(\frac{a}{R}\right)^2 G_2 - 4\left(\frac{a}{R}\right)^3 G_3 \right]$$

G_j : Influence coefficients correspond to the j -th stress distribution

Q : Square root of the complete elliptical integral of the second kind

and is approximated by

$$Q = 1 + 1.464 (a/c)^{1.65}$$

ϕ : Shown in Fig. 7

The K_I can be derived from the above formulas:

$\phi / {}^\circ$	0.0	22.5	45.0	67.5	90.0
$K_I / \text{MPa} \sqrt{\text{m}}$	42.65	46.38	55.38	61.69	63.88

Finite Element Method:

The stress intensity factor K_I calculated using ADINA VCE method is shown in Fig. 7 and compared with the results from analytical and code methods. The comparison is shown that the results from both methods have a good agreement. At the deepest point the K_I from code method is smaller than the results from other two methods, but the safety factor of two is required for K_{Im} calculation in accordance with App. G.

So it was verified that the model in question is reliable and the FEM code, ADINA, is applicable for the fracture mechanics analysis.

5.2 The results from Qinshan SB-LOCA and Rancho Seco

The elastic and elastic-plastic material modes were assumed for the fracture mechanics analysis and the results are shown in Figs 8 and 9 respectively for Qinshan SB-LOCA and Rancho Seco transient. It is observed that the elastic results always are conservative, regardless of the different flaw depth or the different transients. Due to the irradiation effect in EOF the yield strength of the material will enhance. For the condition there is a lack of the irradiated material data in EOF, the elastic results can be used to estimate the fracture behavior of RPV conservatively. The largest K_I occurs at the specific time that the drop rate in temperature is the fastest during the transients and the temperature distributions through the wall thickness are shown in Figs 10 and 11.

For the shallow cracks ($a/w=0.05\sim0.25$), the fracture evaluation are shown in Figs 12 and 13 in comparison with K_{IC} [5]. Based on the ART calculation in EOF in accordance with R.G 1.99 and the screening criterion specified in 10 CFR 50.61, the ART were chosen as 70 °C and 132 °C respectively. It is observed that for the given SB-LOCA the RPV has enough safety margin against the fracture failure even for the most severe postulated Rancho Seco

PTS transient.

The fracture analysis for a series of different flaw depth models ($a/w=0.05\sim0.9$) were performed to investigate the behavior of shallow and deep flaws subject to SB-LOCA and Rancho Seco PTS transients. The K_J vs. a/w at the deepest point of the crack front are described in Fig. 14. The K_J increases with the flaw depth. In order to investigate what kind of flaw is more dangerous the K_{IC} at ART=208 °C and 170 °C were used to compare with the K_J from SB-LOCA and Rancho Seco in Fig. 14. The shallow flaws with the depth $a/w = 0.1\sim0.2$ are more dangerous than others. The distributions of K_J along the crack front are shown in Figs 15 and 16. The same trend were observed for the both conditions that for the base material that the K_J increases with angle ϕ while a/w less than 0.5 and decreases with ϕ while a/w greater than 0.5.

5.3 The results from LB-LOCA

Shown in Fig 5, the LB-LOCA occurs in very short times with the large drop in temperature and pressure. The temperature distribution through the wall thickness is shown in Fig. 17. The two models with $a/w=0.05$ and 0.25 were chosen to perform the fracture analysis under LB-LOCA. The results are shown in Fig. 18 and indicate that the major factor affecting the K_J is the internal pressure for the deep flaws and the drop rate in temperature for the shallow flaws. But the K_J under LB-LOCA is so small that it does not exceed the threshold value of K_{IC} throughout the LB-LOCA transient. Consequently, LB-LOCA is not a dangerous transient for the PTS safety analysis.

5.4 Surface flaw and sub-surface flaw

In this paper sub-surface flaw means the flaw exists behind of the cladding and the depth, a , is the distance from the inner surface to the deepest point of the flaw. The two models with sub-surface flaw ($a/w=0.05$ and 0.25) were performed and compared with the models with surface flaw. The comparison is shown in Figs 19 and 20 at the deepest points of the flaw. It can be estimated how much the results from sub-surface flaw reduce comparing with surface flaw and shown in Table 3. It can be observed that for the sub-surface flaw the K_{Jmax} reduction rate comparing with surface flaw is almost identical for the different PTS transients and a certain a/w and decreases with the flaw

deepening.

Table 3 Comparison between surface flaw and sub-surface flaw

a/w	$K_{J\max}$ / MPa \sqrt{m}				reduction rate	
	surface flaw		sub-surface flaw		S.B.	R.S.
	S.B.	R.S.	S.B.	R.S.	%	%
0.05	43.64	60.58	19.93	27.42	54.33	54.74
0.25	71.73	104.34	50.84	74.21	29.12	28.88

The elastic-plastic calculation always leads to higher K_J of the sub-surface flaw than the linear elastic calculation for the different PTS transients. The comparison is shown in Fig. 21. This rule is very different from the surface flaw.

5.5 Influence of cladding

In the above analyses it was assumed that the cladding always bear the loads along with the base material during the PTS transients. But it was reported that the map cracking existed in cladding before PTS transient occurred. So the supplement analysis was carried out with the conservative assumption that the cladding would be able to conduct heat flux but lose its strength to bear the loads during PTS transient. In order to observe the cladding influence on K_J the two models with $a/w=0.05$ and 0.25 were carried out considering the cladding lost the ability to bear loads and the results are shown in Table 4.

Table 4 Influence of the cladding map cracking (M.C.)

a/w	$K_{J\max}$ / MPa \sqrt{m}	
	without M.C	with M.C
0.05	43.64	30.62
0.25	71.73	87.12

For the shallow flaw ($a/w=0.05$) the map cracking of cladding means to release the constraints for the flaw and K_J would reduce if M.C. exited. But for the deep flaw the surface constraints is so small that it can be omitted and M.C. would reduce the thickness to bear loads leading to increase K_J .

6. Conclusion

- (1) The RPV core betline of Qinshan NPP has enough safety margin to resist the fracture failure under SB-LOCA and idealized Rancho Seco PTS transient in EOF.
- (2) The flaws with depth of $a/w=0.1\sim0.2$ are more dangerous than others during PTS transients.
- (3) LB-LOCA is not a dangerous transient for PTS safety analysis.
- (4) For the surface flaws the elastic calculation always leads to higher K_J than elastic-plastic, but for the sub-surface flaw this rule is reverse.
- (5) For the shallow flaws the map cracking influence can be conservatively ignored but for deep flaws should be considered.

Acknowledgment

The research was carried out in JAERI according to the STA scientist exchange program. I am grateful to my counterpart, the director and the colleagues of my Laboratory for helping me throughout the research. Without their helping I could not complete the research successfully.

Yinbiao HE

Nov., 1999

References

1. American Society of Mechanical Engineers: Boiler and Pressure Vessel Code, Section III, “Nuclear Power Plant Components – Division 1, Appendix G – Protection Against Non Ductile Failure”, New York, (1998) .
2. Code of Federal Regulations: Title 10, Part 50, Section 50.61, “Fracture Toughness Requirements for Protection Against Pressurized Thermal Shock Events”, and Appendix G, “Fracture Toughness Requirements”, Washington, DC, (1996) .
3. U.S. Nuclear Regulatory Commission: “Format and Content of Plant-Specific Pressurized Thermal Shock Safety Analysis Reports for Pressurized Water Reactors”, Regulatory Guide 1.154, Washington, DC, (1987) .
4. U.S. Nuclear Regulatory Commission: “Radiation Embrittlement of Reactor Vessel Materials”, Regulatory Guide 1.99 (Rev. 2), Washington, DC, (1988) .
5. American Society of Mechanical Engineers: Boiler and Pressure Vessel Code, Section XI, “Rules for Inservice Inspection of Nuclear Power Plant Components”, New York, (1998) .
6. ADINA R & D, Inc.: “A Finite Element Program for Automatic Dynamic Incremental Nonlinear Analysis-ADINA/Version 7.2”, (1998) .
7. D. M. Parks: “A Stiffness Derivative Finite Element Technique for Determination of Crack Tip Stress Intensity Factors”, International Journal of Fracture, 10, 487 (1974) .
8. I. S. Raju and J. C. Newman, Jr.: “Stress-Intensity Factor for Internal and External Surface Cracks in Cylindrical Vessels”, Trans. ASME, Ser. J, J. Pressure Vessel Technology, Vol. 104, 293 (1982) .
9. J. C. Newman, Jr. and I. S. Raju: “Stress-Intensity Factor for Internal Surface Cracks in Cylindrical Pressure Vessels”, Trans. ASME, Ser. J, 102, 342, (1980) .
10. J. D. Qu: “Temperature-Pressure Limits of Qinshan 300MW NPP”, SNERDI Technical Report, VSASR-8, (1990) .
11. S. L. Xu et al.: “Design Transients for Qinshan 300MW PWR NPP”, SNERDI Technical Report, (1989) .
12. W. E. Penell: “Heavy Section Steel Technology Program Fracture Issues”, NUREG/CP-0105, (1989) .

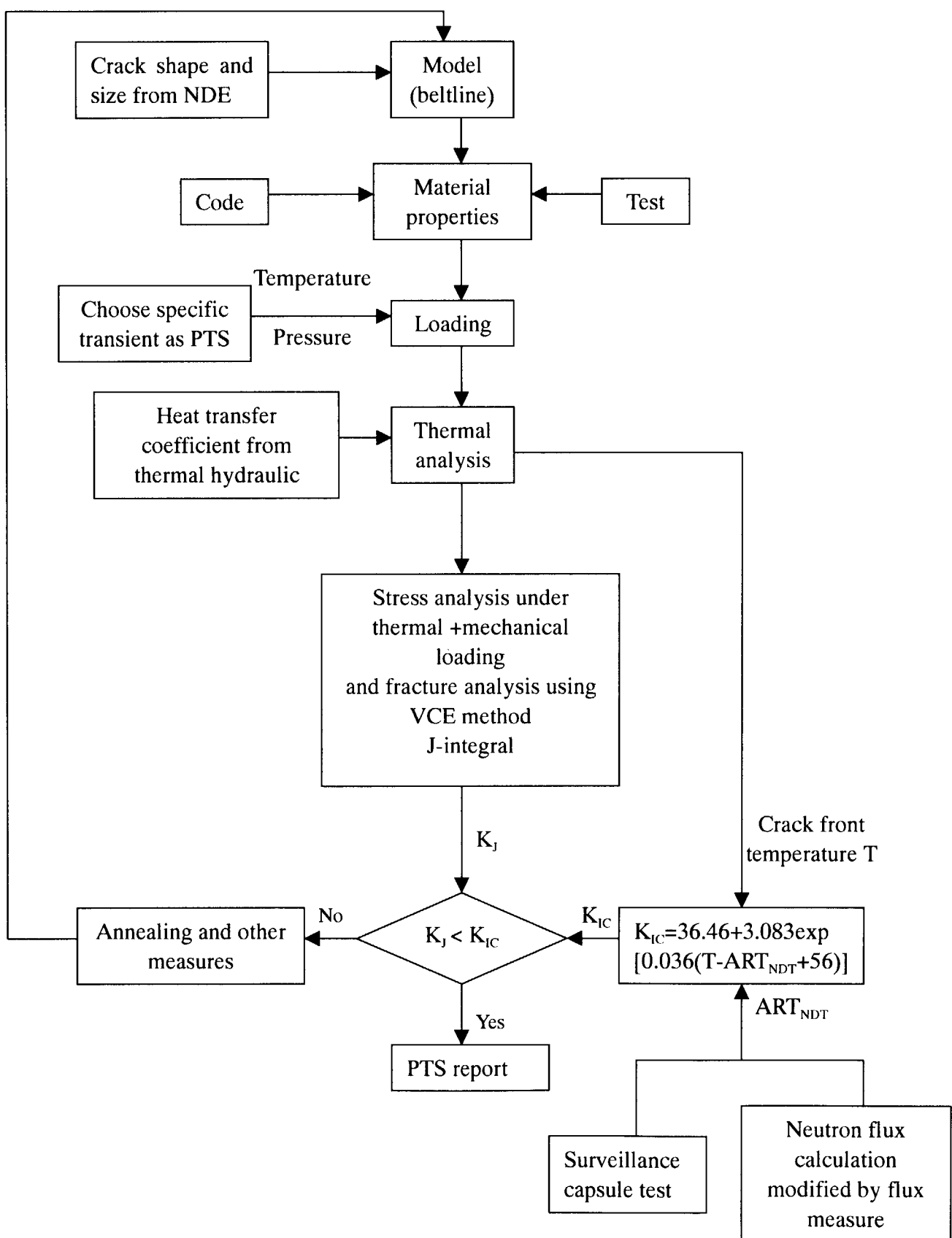


Fig.1 Flow chart of fracture mechanics analysis for beltline of RPV under PTS

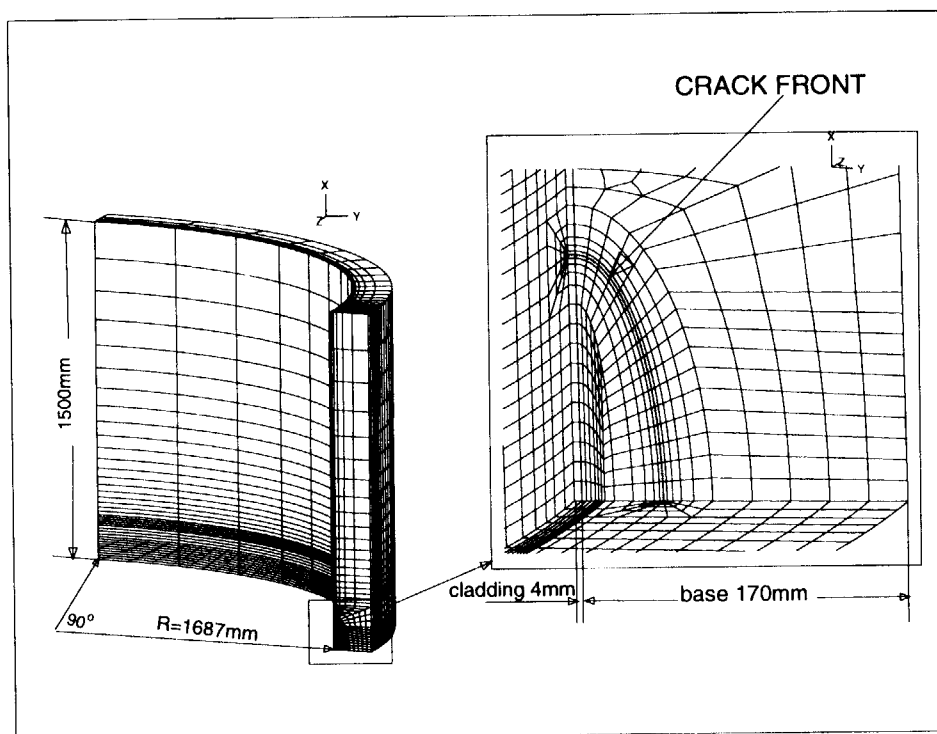


Fig.2 Structural model and mesh

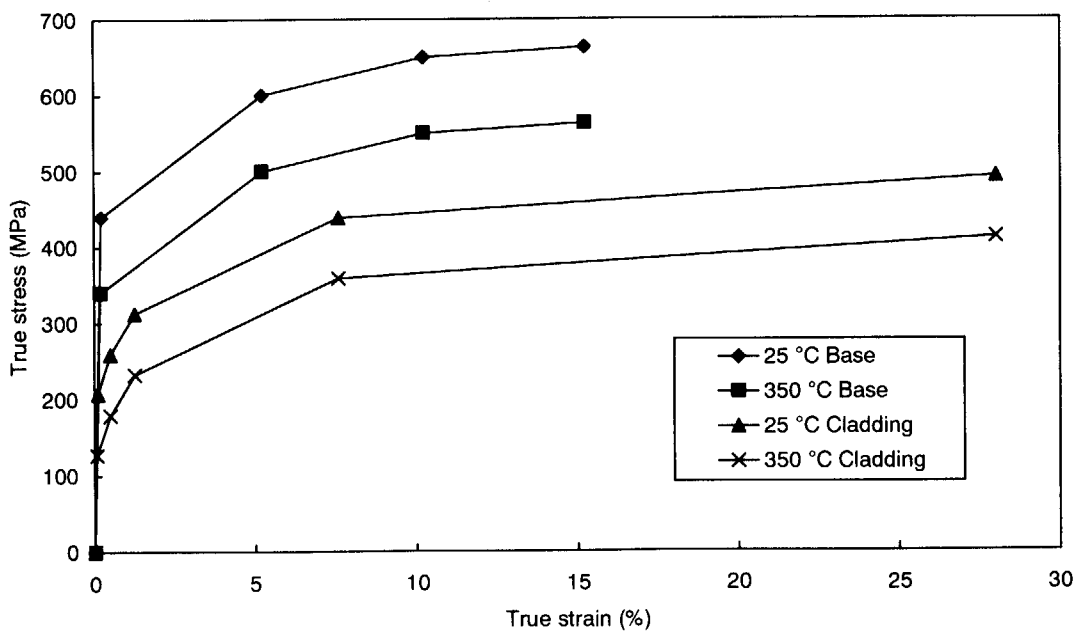


Fig.3 Stress-strain curves in tension for base and cladding

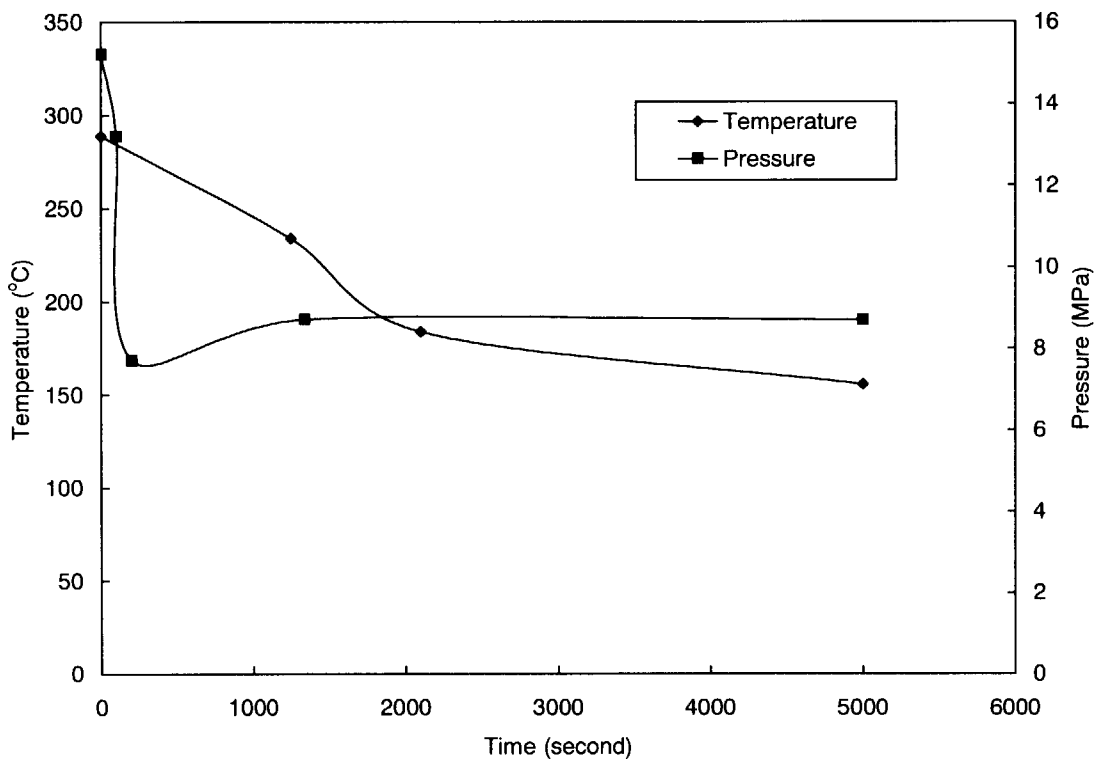


Fig.4 SB-LOCA (SB) transient

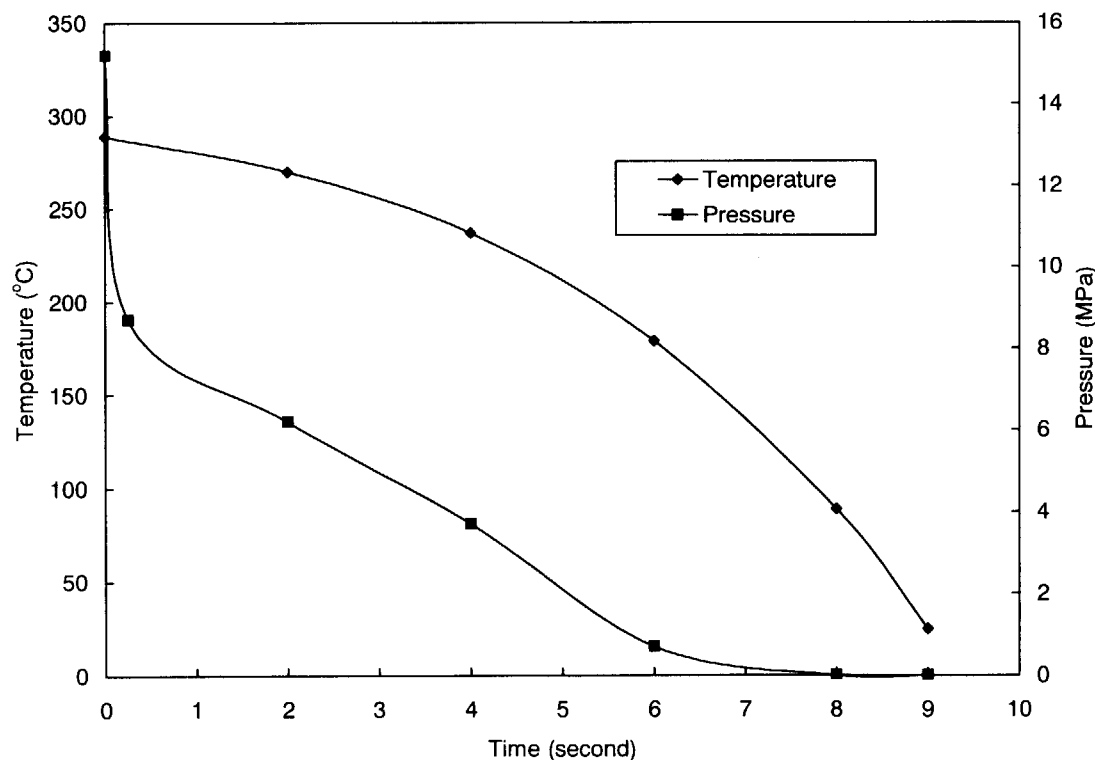


Fig.5 LB-LOCA (LB) transient

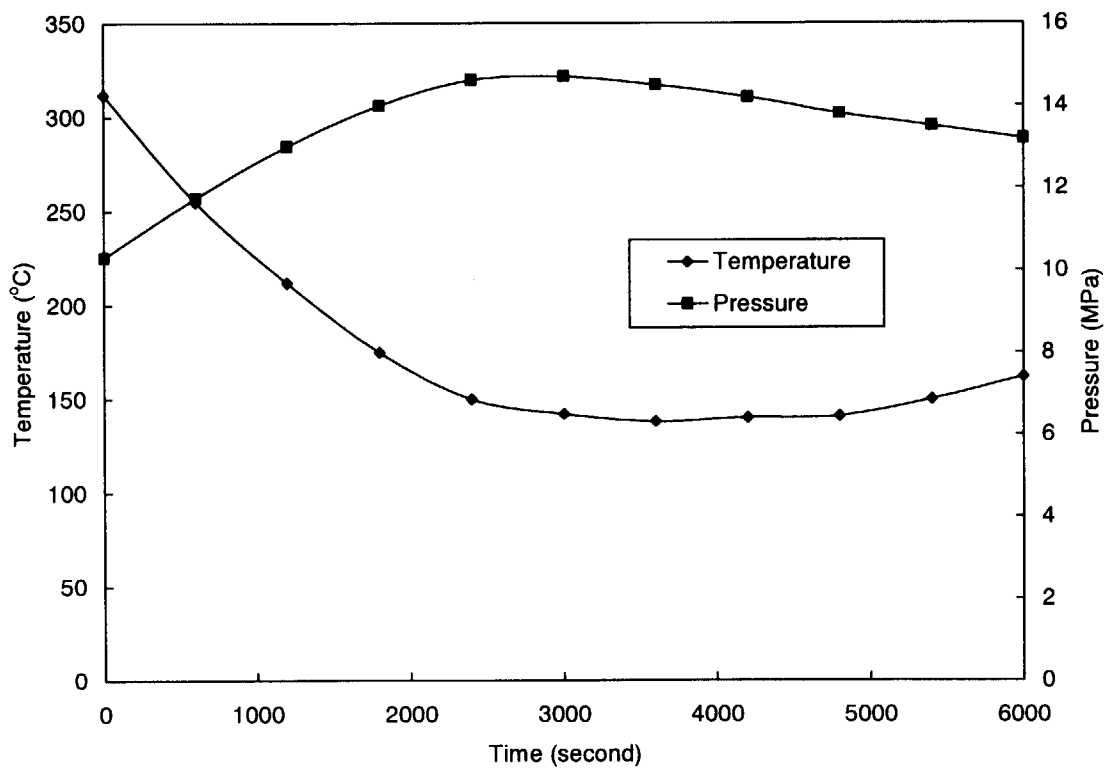


Fig.6 Idealized Rancho Seco (RS) PTS transient

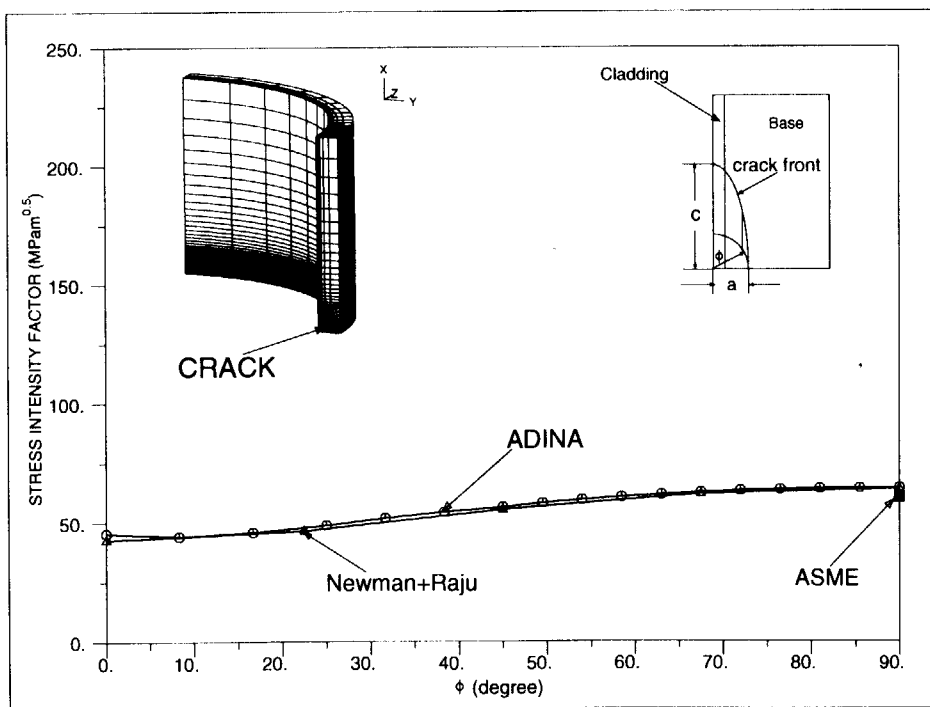


Fig.7 Comparison of stress intensity factor between different methods (no PTS)

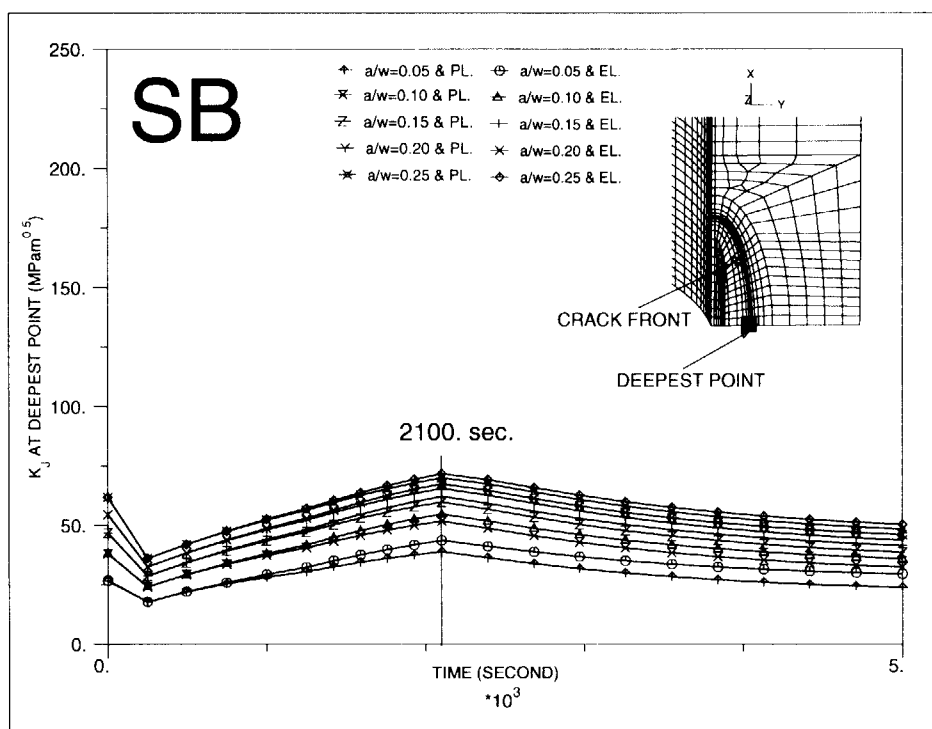


Fig.8 Comparison of K_J between elastic and plastic calculations under SB-LOCA

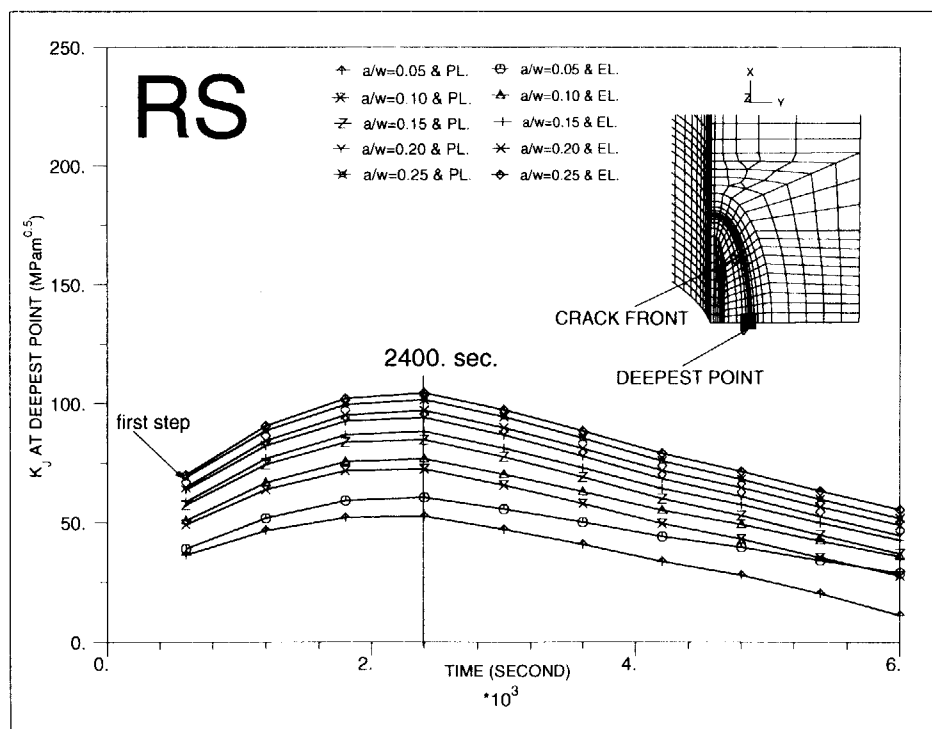


Fig.9 Comparison of K_J between elastic and plastic calculations under RS PTS

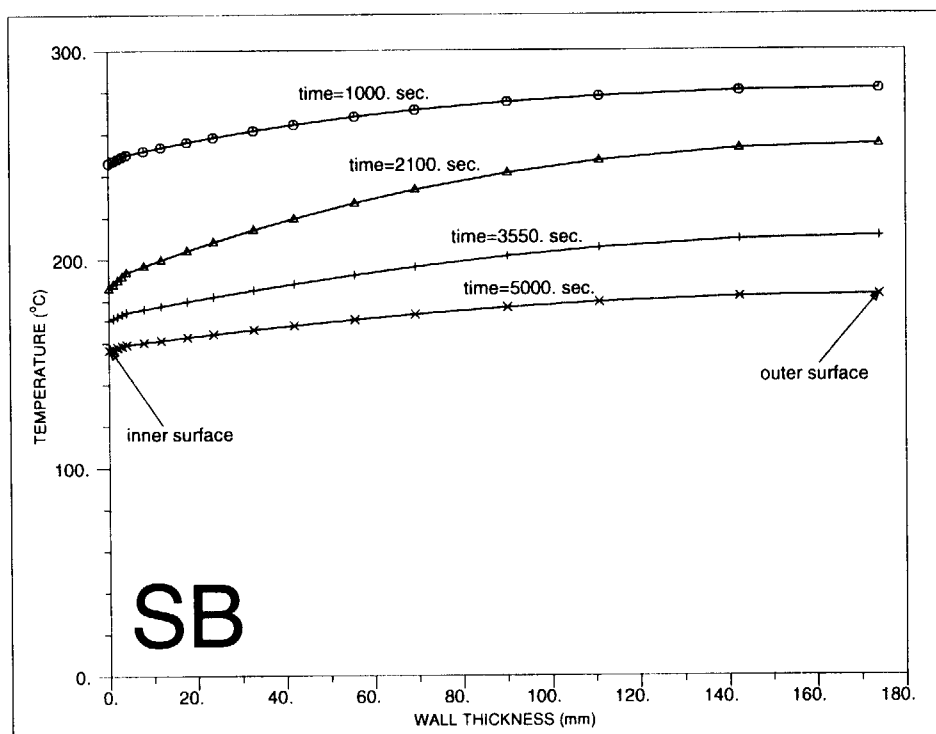


Fig. 10 Temperature distribution through the wall thickness under SB-LOCA

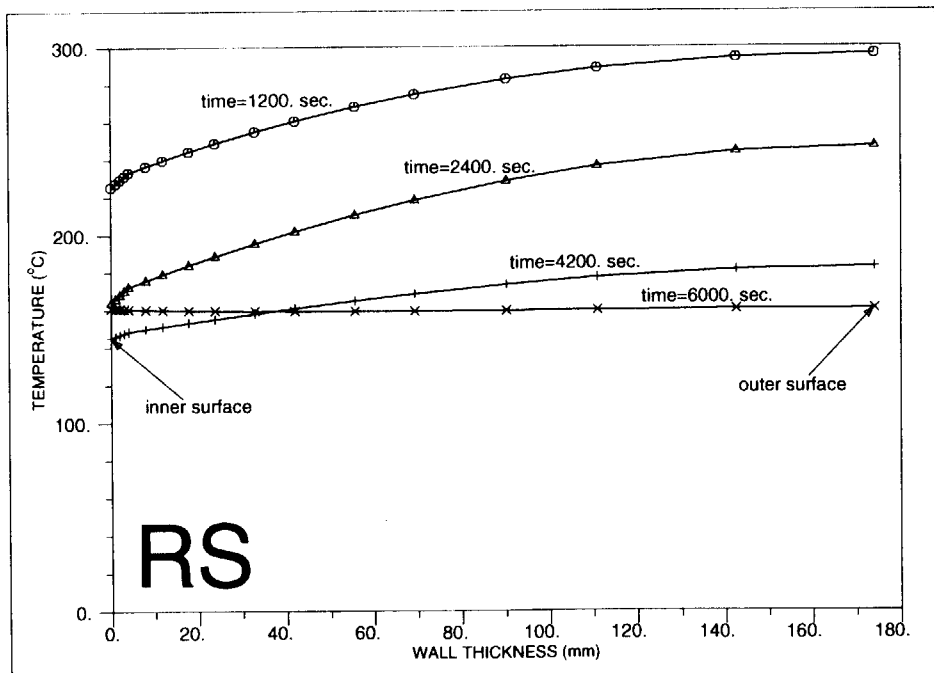


Fig. 11 Temperature distribution through the wall thickness under RS PTS

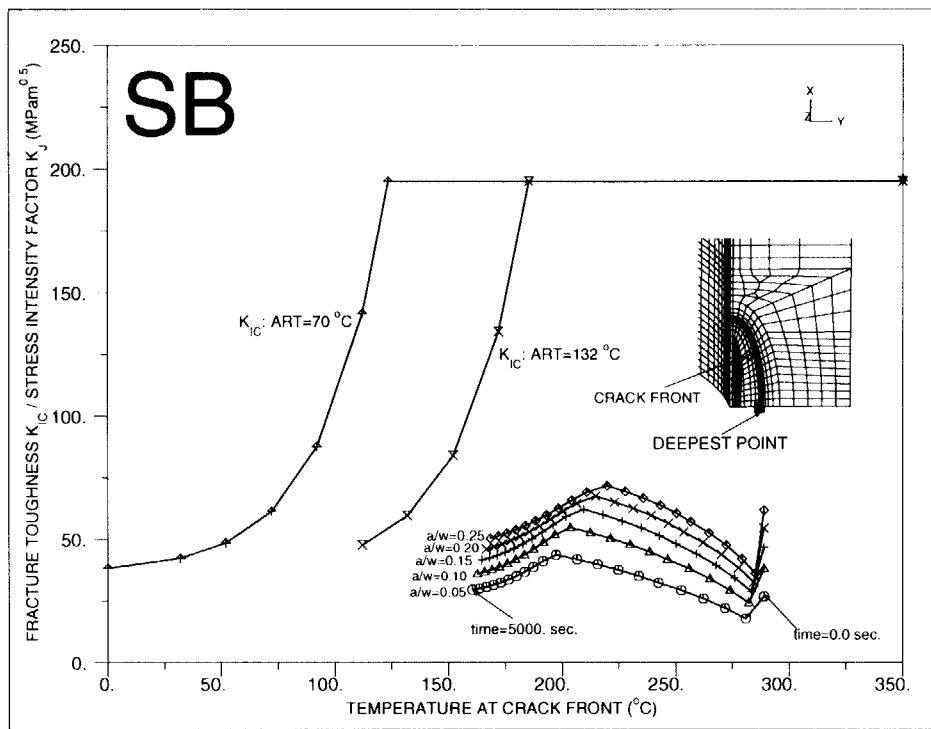


Fig.12 Fracture evaluation for shallow cracks under SB-LOCA

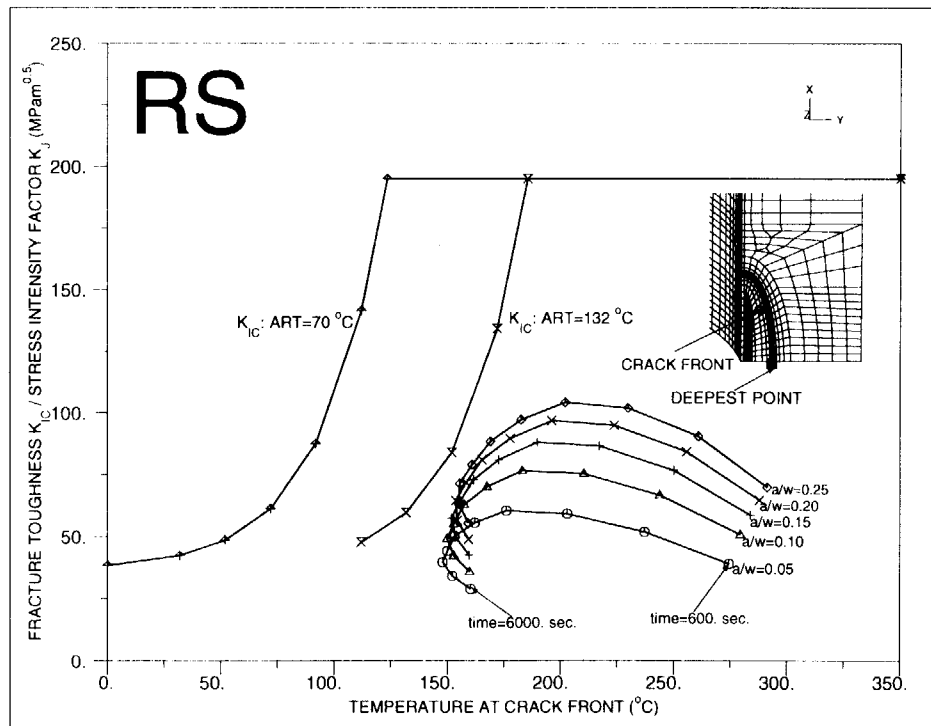


Fig.13 Fracture evaluation for shallow cracks under RS PTS

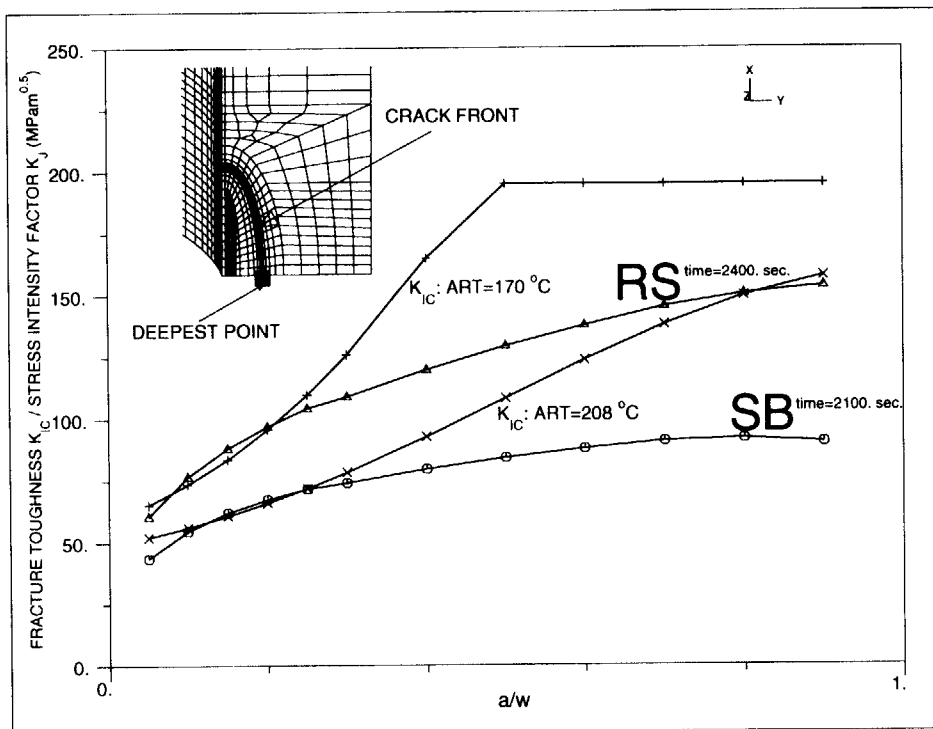


Fig.14 K_J and K_{IC} for different flaws ($a/w=0.05 \sim 0.9$) and PTS transients

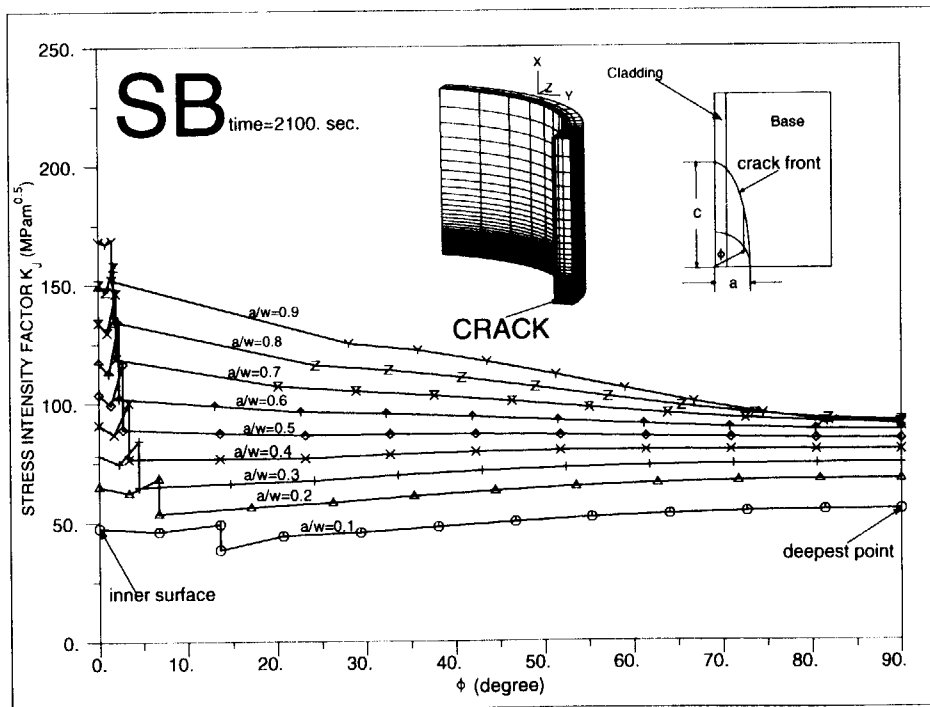


Fig.15 Distribution of K_J along crack front for $a/w=0.1 \sim 0.9$ under SB-LOCA

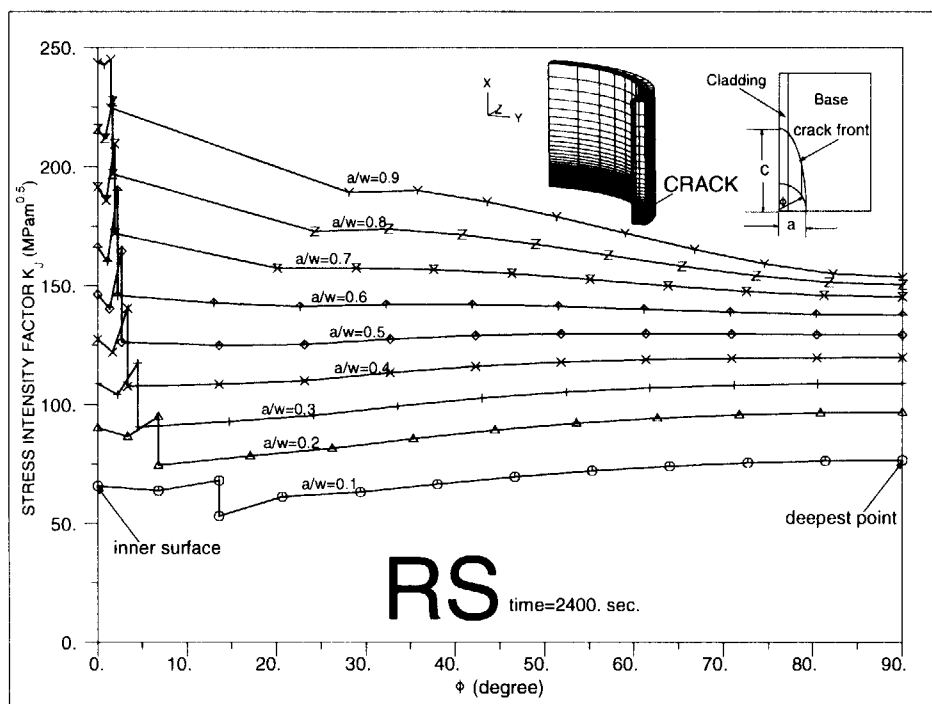


Fig.16 Distribution of K_J along crack front for $a/w=0.1 \sim 0.9$ under RS PTS

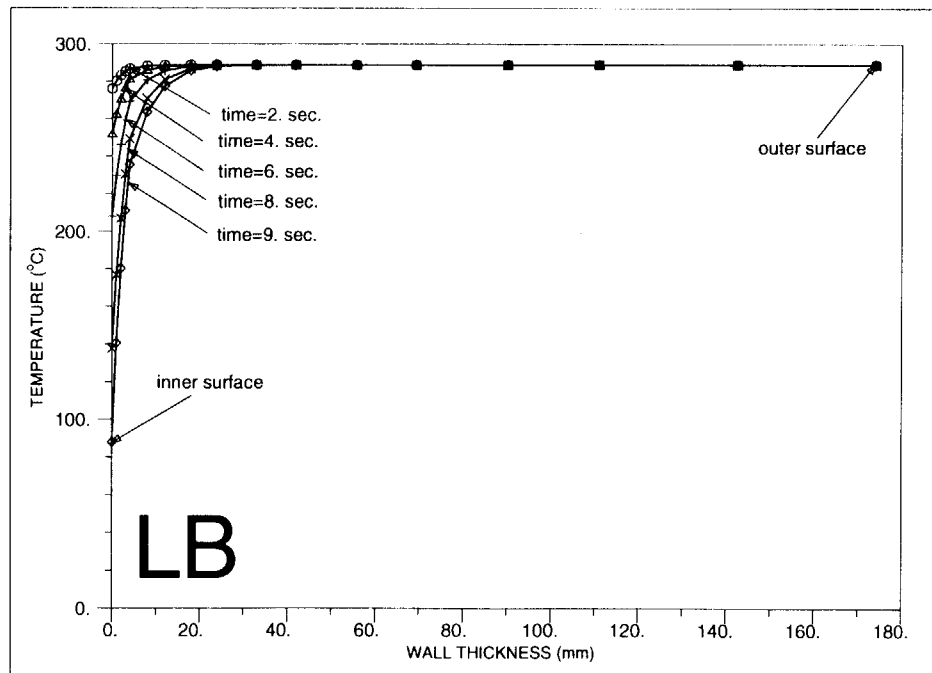


Fig. 17 Temperature distribution through the wall thickness under LB-LOCA

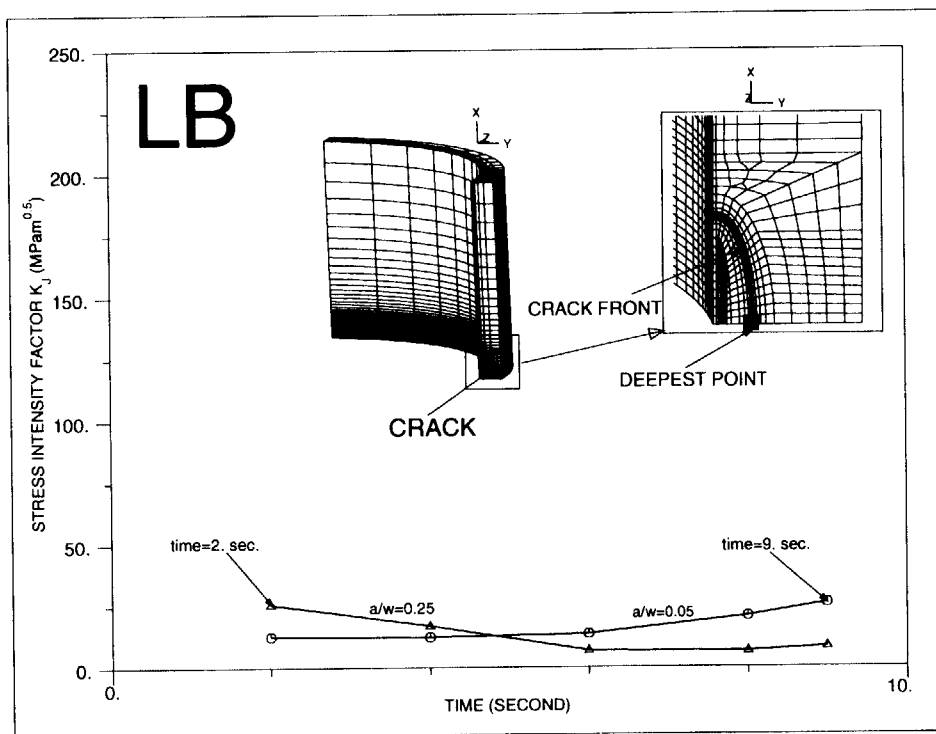


Fig.18 K_J time history under LB-LOCA for $a/w=0.05$ and 0.25

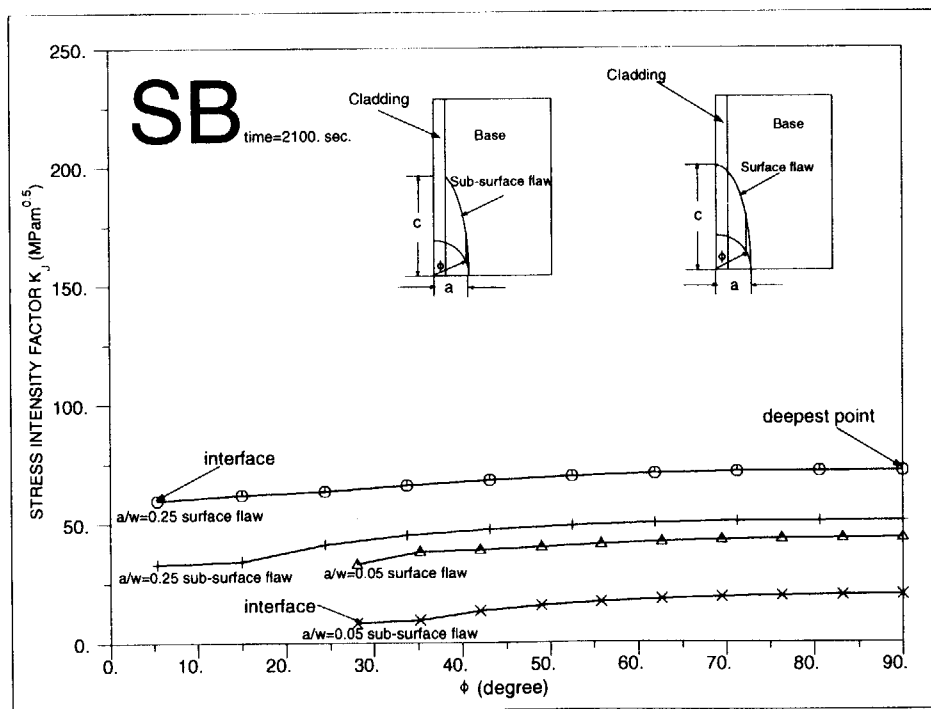


Fig.19 Comparison of K_J between surface and sub-surface flaw under SB-LOCA

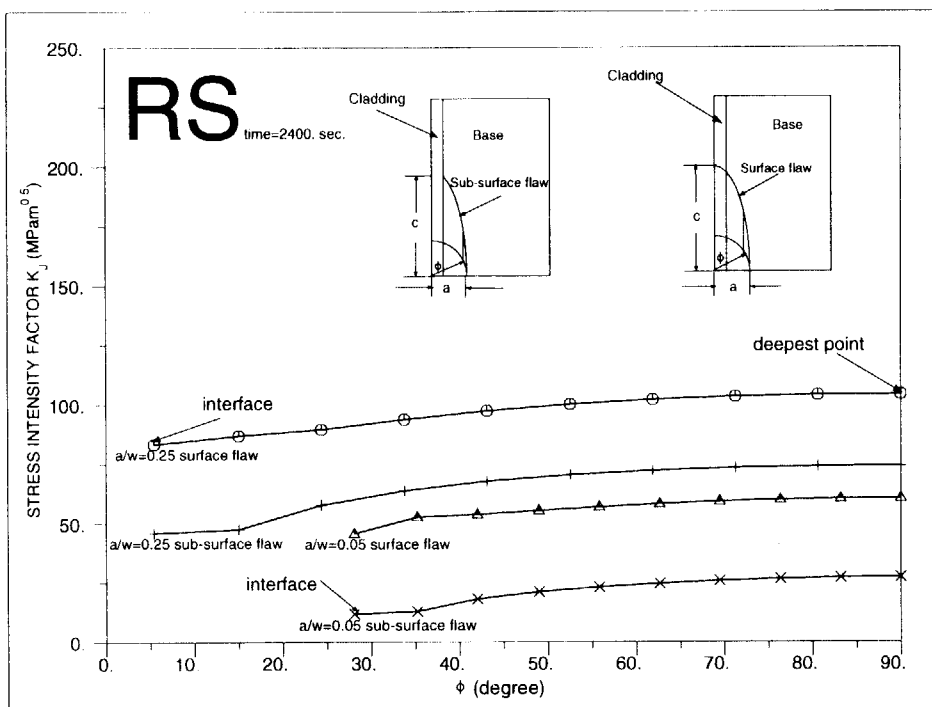


Fig.20 Comparison of K_J between surface and sub-surface flaw under RS PTS

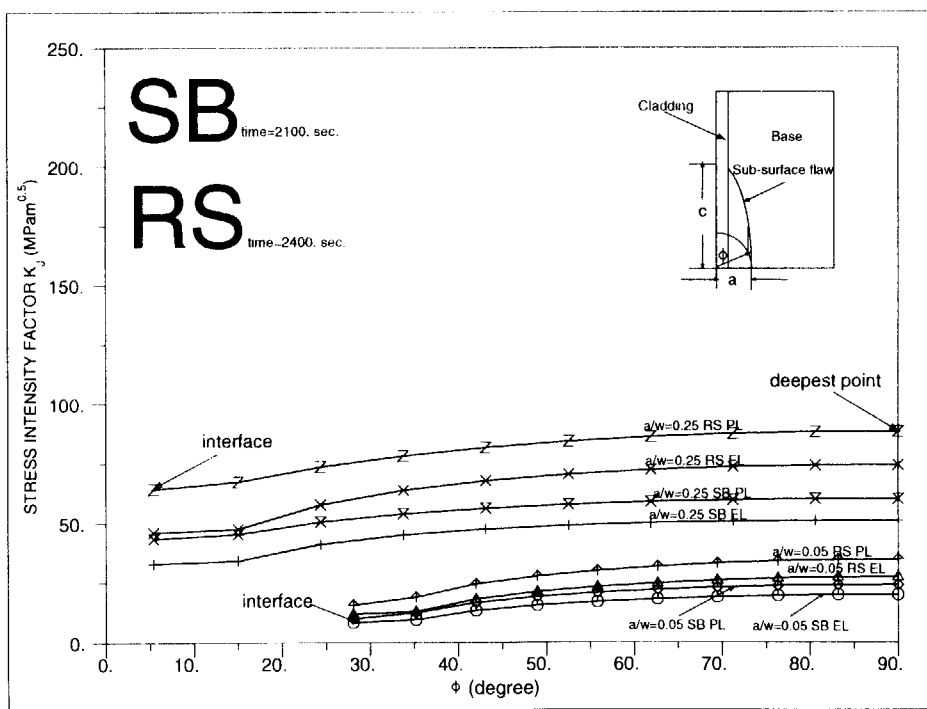


Fig.21 Comparison of K_J between elastic and plastic calculations for sub-surface flaw

Appendix: Data for curve figures

Data for Fig.3 Stress-strain curves in tension for base and cladding

material: base 25 C

true strain	true stress
0.00000E+00	0.00000E+00
2.18905E-01	4.40000E+02
5.21900E+00	6.00000E+02
1.02190E+01	6.50000E+02
1.52190E+01	6.63000E+02

material: base 350 C

true strain	true stress
0.00000E+00	0.00000E+00
1.92090E-01	3.40000E+02
5.21900E+00	5.00000E+02
1.02190E+01	5.50000E+02
1.52190E+01	5.63000E+02

material: cladding 25 C

true strain	true stress
0.00000E+00	0.00000E+00
1.06154E-01	2.07000E+02
5.00000E-01	2.59300E+02
1.25000E+00	3.12500E+02
7.60000E+00	4.38800E+02
2.80000E+01	4.92000E+02

material: cladding 350 C

true strain	true stress
0.00000E+00	0.00000E+00
7.38372E-02	1.27000E+02
5.00000E-01	1.79000E+02
1.25000E+00	2.32500E+02
7.60000E+00	3.58800E+02
2.80000E+01	4.12000E+02

Data for Fig.4 SB-LOCA (SB) transient

time	pressure
------	----------

0.00000E+00	1.52000E+01
1.00000E+02	1.32000E+01
2.00000E+02	7.70000E+00
1.34000E+03	8.70000E+00
5.00000E+03	8.70000E+00

time	temperature
0.00000E+00	2.88800E+02
1.25000E+03	2.33800E+02
2.10000E+03	1.83800E+02
5.00000E+03	1.55800E+02

Data for Fig.5 LB-LOCA (LB) transient

time	pressure
0.00000E+00	1.52000E+01
2.50000E-01	8.70000E+00
2.00000E+00	6.20000E+00
4.00000E+00	3.70000E+00
6.00000E+00	7.00000E-01
8.00000E+00	0.00000E+00
9.00000E+00	0.00000E+00

time	temperature
0.00000E+00	2.88800E+02
2.00000E+00	2.69800E+02
4.00000E+00	2.36800E+02
6.00000E+00	1.78800E+02
8.00000E+00	8.88000E+01
9.00000E+00	2.48000E+01

Data for Fig.6 Idealized Rancho Seco (RS) PTS transient

time	pressure
0.00000E+00	1.03000E+01
6.00000E+02	1.17500E+01
1.20000E+03	1.30000E+01
1.80000E+03	1.40000E+01
2.40000E+03	1.46200E+01
3.00000E+03	1.47000E+01
3.60000E+03	1.45000E+01
4.20000E+03	1.42000E+01

4.80000E+03	1.38000E+01
5.40000E+03	1.35000E+01
6.00000E+03	1.32000E+01

time	temperature
0.00000E+00	3.12000E+02
6.00000E+02	2.55000E+02
1.20000E+03	2.12000E+02
1.80000E+03	1.75000E+02
2.40000E+03	1.50000E+02
3.00000E+03	1.42000E+02
3.60000E+03	1.38000E+02
4.20000E+03	1.40000E+02
4.80000E+03	1.41000E+02
5.40000E+03	1.50000E+02
6.00000E+03	1.62000E+02

Data for Fig.7 Comparison of stress intensity factor between different methods (no PTS)

ADINA

degree	stress intensity factor
0.00000E+00	4.53800E+01
8.33300E+00	4.41900E+01
1.66660E+01	4.58700E+01
2.50000E+01	4.87500E+01
3.16670E+01	5.17800E+01
3.83330E+01	5.43900E+01
4.50000E+01	5.64300E+01
4.95000E+01	5.81400E+01
5.40000E+01	5.94200E+01
5.85000E+01	6.05500E+01
6.30000E+01	6.15300E+01
6.75000E+01	6.23600E+01
7.20000E+01	6.30300E+01
7.65000E+01	6.35600E+01
8.10000E+01	6.39400E+01
8.55000E+01	6.41700E+01
9.00000E+01	6.42400E+01

Newman+Raju

degree	stress intensity factor
0.00000E+00	4.26500E+01
2.25000E+01	4.63800E+01

4.50000E+01	5.53800E+01
6.75000E+01	6.16900E+01
9.00000E+01	6.38800E+01

ASME

degree	stress intensity factor
9.00000E+01	6.02400E+01

Data for Fig.8 Comparison of KJ between elastic and plastic calculations under SB-LOCA

a/w=0.05 & EL.

TIME	KJ
0.00000E+00	2.67800E+01
2.50000E+02	1.77900E+01
5.00000E+02	2.20800E+01
7.50000E+02	2.59100E+01
1.00000E+03	2.93200E+01
1.25000E+03	3.23400E+01
1.42000E+03	3.51000E+01
1.59000E+03	3.75600E+01
1.76000E+03	3.97900E+01
1.93000E+03	4.18100E+01
2.10000E+03	4.36400E+01
2.39000E+03	4.11400E+01
2.68000E+03	3.87700E+01
2.97000E+03	3.67400E+01
3.26000E+03	3.50400E+01
3.55000E+03	3.36300E+01
3.84000E+03	3.24600E+01
4.13000E+03	3.14900E+01
4.42000E+03	3.06900E+01
4.71000E+03	3.00400E+01
5.00000E+03	2.95100E+01

a/w=0.10 & EL.

TIME	KJ
0.00000E+00	3.80500E+01
2.50000E+02	2.41200E+01
5.00000E+02	2.92900E+01
7.50000E+02	3.39600E+01
1.00000E+03	3.80900E+01
1.25000E+03	4.17300E+01
1.42000E+03	4.49200E+01

1.59000E+03	4.77700E+01
1.76000E+03	5.03600E+01
1.93000E+03	5.26700E+01
2.10000E+03	5.47300E+01
2.39000E+03	5.17600E+01
2.68000E+03	4.86900E+01
2.97000E+03	4.59900E+01
3.26000E+03	4.36900E+01
3.55000E+03	4.17700E+01
3.84000E+03	4.01500E+01
4.13000E+03	3.88000E+01
4.42000E+03	3.76700E+01
4.71000E+03	3.67400E+01
5.00000E+03	3.59600E+01

a/w=0.15 & EL.

TIME	KJ
0.00000E+00	4.67800E+01
2.50000E+02	2.87000E+01
5.00000E+02	3.43400E+01
7.50000E+02	3.94900E+01
1.00000E+03	4.40800E+01
1.25000E+03	4.81200E+01
1.42000E+03	5.15300E+01
1.59000E+03	5.46100E+01
1.76000E+03	5.74200E+01
1.93000E+03	5.99200E+01
2.10000E+03	6.21500E+01
2.39000E+03	5.91800E+01
2.68000E+03	5.58300E+01
2.97000E+03	5.28300E+01
3.26000E+03	5.02500E+01
3.55000E+03	4.80800E+01
3.84000E+03	4.62500E+01
4.13000E+03	4.47200E+01
4.42000E+03	4.34400E+01
4.71000E+03	4.23700E+01
5.00000E+03	4.14700E+01

a/w=0.20 & EL.

TIME	KJ
0.00000E+00	5.45100E+01
2.50000E+02	3.25600E+01
5.00000E+02	3.84100E+01

7.50000E+02	4.38300E+01
1.00000E+03	4.86800E+01
1.25000E+03	5.29800E+01
1.42000E+03	5.64600E+01
1.59000E+03	5.96400E+01
1.76000E+03	6.25400E+01
1.93000E+03	6.51400E+01
2.10000E+03	6.74600E+01
2.39000E+03	6.46400E+01
2.68000E+03	6.12200E+01
2.97000E+03	5.80700E+01
3.26000E+03	5.53600E+01
3.55000E+03	5.30500E+01
3.84000E+03	5.11100E+01
4.13000E+03	4.94800E+01
4.42000E+03	4.81200E+01
4.71000E+03	4.69700E+01
5.00000E+03	4.60200E+01

a/w=0.25 & EL.

TIME	KJ
0.00000E+00	6.18000E+01
2.50000E+02	3.60900E+01
5.00000E+02	4.20200E+01
7.50000E+02	4.75900E+01
1.00000E+03	5.26100E+01
1.25000E+03	5.70700E+01
1.42000E+03	6.05800E+01
1.59000E+03	6.37700E+01
1.76000E+03	6.67200E+01
1.93000E+03	6.93700E+01
2.10000E+03	7.17300E+01
2.39000E+03	6.91600E+01
2.68000E+03	6.57900E+01
2.97000E+03	6.26300E+01
3.26000E+03	5.98700E+01
3.55000E+03	5.75200E+01
3.84000E+03	5.55400E+01
4.13000E+03	5.38800E+01
4.42000E+03	5.24900E+01
4.71000E+03	5.13300E+01
5.00000E+03	5.03500E+01

a/w=0.05 & PL.

TIME	KJ
0.00000E+00	2.66000E+01
2.50000E+02	1.77300E+01
5.00000E+02	2.19600E+01
7.50000E+02	2.54100E+01
1.00000E+03	2.81500E+01
1.25000E+03	3.04900E+01
1.42000E+03	3.25700E+01
1.59000E+03	3.44300E+01
1.76000E+03	3.60800E+01
1.93000E+03	3.75600E+01
2.10000E+03	3.88800E+01
2.39000E+03	3.62900E+01
2.68000E+03	3.38100E+01
2.97000E+03	3.16700E+01
3.26000E+03	2.98700E+01
3.55000E+03	2.83600E+01
3.84000E+03	2.71000E+01
4.13000E+03	2.60400E+01
4.42000E+03	2.51700E+01
4.71000E+03	2.44500E+01
5.00000E+03	2.38600E+01

a/w=0.10 & PL.

TIME	KJ
0.00000E+00	3.80400E+01
2.50000E+02	2.40900E+01
5.00000E+02	2.92100E+01
7.50000E+02	3.36200E+01
1.00000E+03	3.73100E+01
1.25000E+03	4.05100E+01
1.42000E+03	4.32800E+01
1.59000E+03	4.57600E+01
1.76000E+03	4.80000E+01
1.93000E+03	4.99800E+01
2.10000E+03	5.17100E+01
2.39000E+03	4.87000E+01
2.68000E+03	4.55600E+01
2.97000E+03	4.28000E+01
3.26000E+03	4.04400E+01
3.55000E+03	3.84500E+01
3.84000E+03	3.67800E+01
4.13000E+03	3.53800E+01
4.42000E+03	3.42000E+01

4.71000E+03	3.32200E+01
5.00000E+03	3.24000E+01

a/w=0.15 & PL.

TIME	KJ
0.00000E+00	4.67700E+01
2.50000E+02	2.86900E+01
5.00000E+02	3.42700E+01
7.50000E+02	3.92200E+01
1.00000E+03	4.34600E+01
1.25000E+03	4.71700E+01
1.42000E+03	5.02400E+01
1.59000E+03	5.30300E+01
1.76000E+03	5.55500E+01
1.93000E+03	5.77900E+01
2.10000E+03	5.97500E+01
2.39000E+03	5.67400E+01
2.68000E+03	5.33500E+01
2.97000E+03	5.03000E+01
3.26000E+03	4.76700E+01
3.55000E+03	4.54500E+01
3.84000E+03	4.35800E+01
4.13000E+03	4.20000E+01
4.42000E+03	4.06800E+01
4.71000E+03	3.95700E+01
5.00000E+03	3.86500E+01

a/w=0.20 & PL.

TIME	KJ
0.00000E+00	5.45200E+01
2.50000E+02	3.25400E+01
5.00000E+02	3.83400E+01
7.50000E+02	4.36100E+01
1.00000E+03	4.81700E+01
1.25000E+03	5.21800E+01
1.42000E+03	5.54000E+01
1.59000E+03	5.83300E+01
1.76000E+03	6.10000E+01
1.93000E+03	6.33800E+01
2.10000E+03	6.54700E+01
2.39000E+03	6.26400E+01
2.68000E+03	5.91800E+01
2.97000E+03	5.60000E+01
3.26000E+03	5.32400E+01

3.55000E+03	5.09000E+01
3.84000E+03	4.89200E+01
4.13000E+03	4.72600E+01
4.42000E+03	4.58600E+01
4.71000E+03	4.46900E+01
5.00000E+03	4.37000E+01

a/w=0.25 & PL.

TIME	KJ
0.00000E+00	6.18300E+01
2.50000E+02	3.60700E+01
5.00000E+02	4.19600E+01
7.50000E+02	4.74200E+01
1.00000E+03	5.21800E+01
1.25000E+03	5.63800E+01
1.42000E+03	5.96400E+01
1.59000E+03	6.26100E+01
1.76000E+03	6.53500E+01
1.93000E+03	6.77800E+01
2.10000E+03	6.99400E+01
2.39000E+03	6.73700E+01
2.68000E+03	6.39700E+01
2.97000E+03	6.07800E+01
3.26000E+03	5.80000E+01
3.55000E+03	5.56200E+01
3.84000E+03	5.36200E+01
4.13000E+03	5.19300E+01
4.42000E+03	5.05200E+01
4.71000E+03	4.93300E+01
5.00000E+03	4.83300E+01

Data for Fig.9 Comparison of KJ between elastic and plastic calculations under RS PTS

a/w=0.05 & EL.

TIME	KJ
6.00000E+02	3.90100E+01
1.20000E+03	5.19200E+01
1.80000E+03	5.92800E+01
2.40000E+03	6.05800E+01
3.00000E+03	5.57100E+01
3.60000E+03	5.02400E+01
4.20000E+03	4.42300E+01
4.80000E+03	3.97100E+01

5.40000E+03	3.41700E+01
6.00000E+03	2.89200E+01

a/w=0.10 & EL.

TIME	KJ
6.00000E+02	5.08100E+01
1.20000E+03	6.68000E+01
1.80000E+03	7.55600E+01
2.40000E+03	7.67300E+01
3.00000E+03	7.03000E+01
3.60000E+03	6.30300E+01
4.20000E+03	5.52200E+01
4.80000E+03	4.92500E+01
5.40000E+03	4.23200E+01
6.00000E+03	3.58100E+01

a/w=0.15 & EL.

TIME	KJ
6.00000E+02	5.87200E+01
1.20000E+03	7.68200E+01
1.80000E+03	8.67400E+01
2.40000E+03	8.82100E+01
3.00000E+03	8.12100E+01
3.60000E+03	7.30600E+01
4.20000E+03	6.43500E+01
4.80000E+03	5.75700E+01
5.40000E+03	4.99000E+01
6.00000E+03	4.27000E+01

a/w=0.20 & EL.

TIME	KJ
6.00000E+02	6.47900E+01
1.20000E+03	8.43100E+01
1.80000E+03	9.50800E+01
2.40000E+03	9.69300E+01
3.00000E+03	8.97500E+01
3.60000E+03	8.11500E+01
4.20000E+03	7.19400E+01
4.80000E+03	6.46600E+01
5.40000E+03	5.66000E+01
6.00000E+03	4.90100E+01

a/w=0.25 & EL.

TIME	KJ
------	----

6.00000E+02	6.99800E+01
1.20000E+03	9.05300E+01
1.80000E+03	1.02030E+02
2.40000E+03	1.04330E+02
3.00000E+03	9.72800E+01
3.60000E+03	8.85100E+01
4.20000E+03	7.91000E+01
4.80000E+03	7.15100E+01
5.40000E+03	6.32800E+01
6.00000E+03	5.54800E+01

a/w=0.05 & PL.

TIME	KJ
6.00000E+02	3.64000E+01
1.20000E+03	4.67000E+01
1.80000E+03	5.21100E+01
2.40000E+03	5.26500E+01
3.00000E+03	4.71600E+01
3.60000E+03	4.08700E+01
4.20000E+03	3.37100E+01
4.80000E+03	2.79700E+01
5.40000E+03	2.03200E+01
6.00000E+03	1.12300E+01

a/w=0.10 & PL.

TIME	KJ
6.00000E+02	4.91600E+01
1.20000E+03	6.39000E+01
1.80000E+03	7.17800E+01
2.40000E+03	7.24500E+01
3.00000E+03	6.57100E+01
3.60000E+03	5.80100E+01
4.20000E+03	4.96600E+01
4.80000E+03	4.31200E+01
5.40000E+03	3.53500E+01
6.00000E+03	2.77500E+01

a/w=0.15 & PL.

TIME	KJ
6.00000E+02	5.74000E+01
1.20000E+03	7.44000E+01
1.80000E+03	8.36900E+01
2.40000E+03	8.47000E+01
3.00000E+03	7.75800E+01

3.60000E+03	6.91600E+01
4.20000E+03	6.01000E+01
4.80000E+03	5.29500E+01
5.40000E+03	4.48100E+01
6.00000E+03	3.70000E+01

a/w=0.20 & PL.

TIME	KJ
6.00000E+02	6.37100E+01
1.20000E+03	8.22300E+01
1.80000E+03	9.25000E+01
2.40000E+03	9.39800E+01
3.00000E+03	8.67300E+01
3.60000E+03	7.79300E+01
4.20000E+03	6.85000E+01
4.80000E+03	6.09500E+01
5.40000E+03	5.26000E+01
6.00000E+03	4.46400E+01

a/w=0.25 & PL.

TIME	KJ
6.00000E+02	6.90000E+01
1.20000E+03	8.85200E+01
1.80000E+03	9.94400E+01
2.40000E+03	1.01480E+02
3.00000E+03	9.43300E+01
3.60000E+03	8.54500E+01
4.20000E+03	7.59100E+01
4.80000E+03	6.81700E+01
5.40000E+03	5.98000E+01
6.00000E+03	5.18300E+01

Data for Fig.10 Temperature distribution through the wall thickness under SB-LOCA

time=1000. sec.

WALL THICKNESS	TEMPERATURE
0.00000E+00	2.46100E+02
1.00000E+00	2.47157E+02
2.00000E+00	2.48201E+02
3.00000E+00	2.49232E+02
4.00000E+00	2.50252E+02
4.00100E+00	2.50252E+02
7.94102E+00	2.52019E+02

1.18810E+01	2.53715E+02
1.78530E+01	2.56154E+02
2.38250E+01	2.58439E+02
3.28768E+01	2.61625E+02
4.19286E+01	2.64494E+02
5.56485E+01	2.68287E+02
6.93685E+01	2.71473E+02
9.01640E+01	2.75284E+02
1.10960E+02	2.78040E+02
1.42480E+02	2.80546E+02
1.74000E+02	2.81336E+02

time=2100. sec.

WALL THICKNESS	TEMPERATURE
0.00000E+00	1.86061E+02
1.00000E+00	1.88016E+02
2.00000E+00	1.89953E+02
3.00000E+00	1.91870E+02
4.00000E+00	1.93768E+02
4.00100E+00	1.93768E+02
7.94102E+00	1.96843E+02
1.18810E+01	1.99822E+02
1.78530E+01	2.04159E+02
2.38250E+01	2.08286E+02
3.28768E+01	2.14149E+02
4.19286E+01	2.19555E+02
5.56485E+01	2.26909E+02
6.93685E+01	2.33298E+02
9.01640E+01	2.41251E+02
1.10960E+02	2.47258E+02
1.42480E+02	2.52948E+02
1.74000E+02	2.54798E+02

time=3550. sec.

WALL THICKNESS	TEMPERATURE
0.00000E+00	1.70883E+02
1.00000E+00	1.71835E+02
2.00000E+00	1.72782E+02
3.00000E+00	1.73726E+02
4.00000E+00	1.74665E+02
4.00100E+00	1.74665E+02
7.94102E+00	1.76176E+02
1.18810E+01	1.77664E+02
1.78530E+01	1.79874E+02

2.38250E+01	1.82029E+02
3.28768E+01	1.85180E+02
4.19286E+01	1.88186E+02
5.56485E+01	1.92442E+02
6.93685E+01	1.96312E+02
9.01640E+01	2.01377E+02
1.10960E+02	2.05409E+02
1.42480E+02	2.09407E+02
1.74000E+02	2.10751E+02

time=5000. sec.

WALL THICKNESS	TEMPERATURE
0.00000E+00	1.56543E+02
1.00000E+00	1.57204E+02
2.00000E+00	1.57862E+02
3.00000E+00	1.58516E+02
4.00000E+00	1.59167E+02
4.00100E+00	1.59167E+02
7.94102E+00	1.60195E+02
1.18810E+01	1.61204E+02
1.78530E+01	1.62696E+02
2.38250E+01	1.64143E+02
3.28768E+01	1.66246E+02
4.19286E+01	1.68237E+02
5.56485E+01	1.71034E+02
6.93685E+01	1.73555E+02
9.01640E+01	1.76824E+02
1.10960E+02	1.79402E+02
1.42480E+02	1.81939E+02
1.74000E+02	1.82787E+02

Data for Fig.11 Temperature distribution through the wall thickness under RS PTS

time=1200. sec.

WALL THICKNESS	TEMPERATURE
0.00000E+00	2.25465E+02
1.00000E+00	2.27463E+02
2.00000E+00	2.29440E+02
3.00000E+00	2.31393E+02
4.00000E+00	2.33325E+02
4.00100E+00	2.33325E+02
7.94102E+00	2.36613E+02
1.18810E+01	2.39790E+02

1.78530E+01	2.44397E+02
2.38250E+01	2.48761E+02
3.28768E+01	2.54923E+02
4.19286E+01	2.60563E+02
5.56485E+01	2.68161E+02
6.93685E+01	2.74684E+02
9.01640E+01	2.82684E+02
1.10960E+02	2.88623E+02
1.42480E+02	2.94152E+02
1.74000E+02	2.95926E+02

time=2400. sec.

WALL THICKNESS	TEMPERATURE
0.00000E+00	1.63735E+02
1.00000E+00	1.65902E+02
2.00000E+00	1.68052E+02
3.00000E+00	1.70185E+02
4.00000E+00	1.72301E+02
4.00100E+00	1.72301E+02
7.94102E+00	1.75678E+02
1.18810E+01	1.78980E+02
1.78530E+01	1.83839E+02
2.38250E+01	1.88521E+02
3.28768E+01	1.95282E+02
4.19286E+01	2.01631E+02
5.56485E+01	2.10473E+02
6.93685E+01	2.18364E+02
9.01640E+01	2.28486E+02
1.10960E+02	2.36374E+02
1.42480E+02	2.44055E+02
1.74000E+02	2.46603E+02

time=4200. sec.

WALL THICKNESS	TEMPERATURE
0.00000E+00	1.45215E+02
1.00000E+00	1.46055E+02
2.00000E+00	1.46894E+02
3.00000E+00	1.47730E+02
4.00000E+00	1.48564E+02
4.00100E+00	1.48564E+02
7.94102E+00	1.49878E+02
1.18810E+01	1.51182E+02
1.78530E+01	1.53138E+02
2.38250E+01	1.55065E+02

3.28768E+01	1.57917E+02
4.19286E+01	1.60673E+02
5.56485E+01	1.64633E+02
6.93685E+01	1.68286E+02
9.01640E+01	1.73138E+02
1.10960E+02	1.77051E+02
1.42480E+02	1.80970E+02
1.74000E+02	1.82297E+02

time=6000. sec.

WALL THICKNESS	TEMPERATURE
0.00000E+00	1.61011E+02
1.00000E+00	1.60857E+02
2.00000E+00	1.60706E+02
3.00000E+00	1.60560E+02
4.00000E+00	1.60419E+02
4.00100E+00	1.60419E+02
7.94102E+00	1.60207E+02
1.18810E+01	1.60019E+02
1.78530E+01	1.59774E+02
2.38250E+01	1.59576E+02
3.28768E+01	1.59354E+02
4.19286E+01	1.59215E+02
5.56485E+01	1.59132E+02
6.93685E+01	1.59167E+02
9.01640E+01	1.59361E+02
1.10960E+02	1.59628E+02
1.42480E+02	1.59984E+02
1.74000E+02	1.60125E+02

Data for Fig.12 Fracture evaluation for shallow cracks under SB-LOCA

a/w=0.05

TEMPERATURE	KJ
2.88800E+02	2.67800E+01
2.80870E+02	1.77900E+01
2.71710E+02	2.20800E+01
2.62110E+02	2.59100E+01
2.52260E+02	2.93200E+01
2.42250E+02	3.23400E+01
2.33760E+02	3.51000E+01
2.24840E+02	3.75600E+01
2.15750E+02	3.97900E+01

2.06560E+02	4.18100E+01
1.97270E+02	4.36400E+01
1.91600E+02	4.11400E+01
1.87320E+02	3.87700E+01
1.83480E+02	3.67400E+01
1.79860E+02	3.50400E+01
1.76390E+02	3.36300E+01
1.73030E+02	3.24600E+01
1.69750E+02	3.14900E+01
1.66560E+02	3.06900E+01
1.63420E+02	3.00400E+01
1.60340E+02	2.95100E+01

a/w=0.10

TEMPERATURE	KJ
2.88800E+02	3.80500E+01
2.82210E+02	2.41200E+01
2.73970E+02	2.92900E+01
2.65080E+02	3.39600E+01
2.55820E+02	3.80900E+01
2.46280E+02	4.17300E+01
2.38440E+02	4.49200E+01
2.30020E+02	4.77700E+01
2.21350E+02	5.03600E+01
2.12520E+02	5.26700E+01
2.03550E+02	5.47300E+01
1.96750E+02	5.17600E+01
1.91760E+02	4.86900E+01
1.87400E+02	4.59900E+01
1.83370E+02	4.36900E+01
1.79560E+02	4.17700E+01
1.75920E+02	4.01500E+01
1.72410E+02	3.88000E+01
1.69010E+02	3.76700E+01
1.65710E+02	3.67400E+01
1.62490E+02	3.59600E+01

a/w=0.15

TEMPERATURE	KJ
2.88800E+02	4.67800E+01
2.83320E+02	2.87000E+01
2.75950E+02	3.43400E+01
2.67750E+02	3.94900E+01
2.59050E+02	4.40800E+01

2.49990E+02	4.81200E+01
2.42720E+02	5.15300E+01
2.34790E+02	5.46100E+01
2.26530E+02	5.74200E+01
2.18060E+02	5.99200E+01
2.09400E+02	6.21500E+01
2.01690E+02	5.91800E+01
1.96050E+02	5.58300E+01
1.91190E+02	5.28300E+01
1.86760E+02	5.02500E+01
1.82620E+02	4.80800E+01
1.78700E+02	4.62500E+01
1.74960E+02	4.47200E+01
1.71370E+02	4.34400E+01
1.67900E+02	4.23700E+01
1.64540E+02	4.14700E+01

a/w=0.20

TEMPERATURE	KJ
2.88800E+02	5.45100E+01
2.84240E+02	3.25600E+01
2.77690E+02	3.84100E+01
2.70150E+02	4.38300E+01
2.62000E+02	4.86800E+01
2.53400E+02	5.29800E+01
2.46640E+02	5.64600E+01
2.39170E+02	5.96400E+01
2.31320E+02	6.25400E+01
2.23190E+02	6.51400E+01
2.14840E+02	6.74600E+01
2.06420E+02	6.46400E+01
2.00160E+02	6.12200E+01
1.94840E+02	5.80700E+01
1.90020E+02	5.53600E+01
1.85560E+02	5.30500E+01
1.81370E+02	5.11100E+01
1.77400E+02	4.94800E+01
1.73620E+02	4.81200E+01
1.69990E+02	4.69700E+01
1.66500E+02	4.60200E+01

a/w=0.25

TEMPERATURE	KJ
2.88800E+02	6.18000E+01

2.85010E+02	3.60900E+01
2.79190E+02	4.20200E+01
2.72290E+02	4.75900E+01
2.64660E+02	5.26100E+01
2.56510E+02	5.70700E+01
2.50210E+02	6.05800E+01
2.43180E+02	6.37700E+01
2.35710E+02	6.67200E+01
2.27930E+02	6.93700E+01
2.19880E+02	7.17300E+01
2.10900E+02	6.91600E+01
2.04100E+02	6.57900E+01
1.98320E+02	6.26300E+01
1.93140E+02	5.98700E+01
1.88370E+02	5.75200E+01
1.83920E+02	5.55400E+01
1.79730E+02	5.38800E+01
1.75770E+02	5.24900E+01
1.71980E+02	5.13300E+01
1.68360E+02	5.03500E+01

KIC: ART=70 C

TEMPERATURE	KIC
0.00000E+00	3.83200E+01
3.20000E+01	4.23500E+01
5.20000E+01	4.85700E+01
7.20000E+01	6.13400E+01
9.20000E+01	8.75700E+01
1.12000E+02	1.41450E+02
1.23448E+02	1.95000E+02
3.50000E+02	1.95000E+02

KIC: ART=132 C

TEMPERATURE	KIC
1.12000E+02	4.77300E+01
1.32000E+02	5.96100E+01
1.52000E+02	8.40200E+01
1.72000E+02	1.34160E+02
1.85448E+02	1.95000E+02
3.50000E+02	1.95000E+02

Data for Fig.13 Fracture evaluation for shallow cracks under RS PTS

a/w=0.05

TEMPERATURE	KJ
2.74480E+02	3.90100E+01
2.37070E+02	5.19200E+01
2.02890E+02	5.92800E+01
1.76150E+02	6.05800E+01
1.62070E+02	5.57100E+01
1.53240E+02	5.02400E+01
1.50060E+02	4.42300E+01
1.47990E+02	3.97100E+01
1.52170E+02	3.41700E+01
1.60180E+02	2.89200E+01

a/w=0.10

TEMPERATURE	KJ
2.79500E+02	5.08100E+01
2.43760E+02	6.68000E+01
2.10320E+02	7.55600E+01
1.83160E+02	7.67300E+01
1.67530E+02	7.03000E+01
1.57400E+02	6.30300E+01
1.52860E+02	5.52200E+01
1.49930E+02	4.92500E+01
1.52870E+02	4.23200E+01
1.59810E+02	3.58100E+01

a/w=0.15

TEMPERATURE	KJ
2.83940E+02	5.87200E+01
2.49940E+02	7.68200E+01
2.17300E+02	8.67400E+01
1.89800E+02	8.82100E+01
1.72800E+02	8.12100E+01
1.61430E+02	7.30600E+01
1.55600E+02	6.43500E+01
1.51830E+02	5.75700E+01
1.53600E+02	4.99000E+01
1.59530E+02	4.27000E+01

a/w=0.20

TEMPERATURE	KJ
2.87860E+02	6.47900E+01
2.55650E+02	8.43100E+01
2.23830E+02	9.50800E+01

1.96090E+02	9.69300E+01
1.77840E+02	8.97500E+01
1.65310E+02	8.11500E+01
1.58260E+02	7.19400E+01
1.53680E+02	6.46600E+01
1.54370E+02	5.66000E+01
1.59330E+02	4.90100E+01

a/w=0.25

TEMPERATURE	KJ
2.91290E+02	6.99800E+01
2.60900E+02	9.05300E+01
2.29920E+02	1.02030E+02
2.02010E+02	1.04340E+02
1.82660E+02	9.72800E+01
1.69030E+02	8.85100E+01
1.60840E+02	7.91000E+01
1.55460E+02	7.15100E+01
1.55160E+02	6.32800E+01
1.59210E+02	5.54800E+01

KIC: ART=70 C

TEMPERATURE	KIC
0.00000E+00	3.83200E+01
3.20000E+01	4.23500E+01
5.20000E+01	4.85700E+01
7.20000E+01	6.13400E+01
9.20000E+01	8.75700E+01
1.12000E+02	1.41450E+02
1.23448E+02	1.95000E+02
3.50000E+02	1.95000E+02

KIC: ART=132 C

TEMPERATURE	KIC
1.12000E+02	4.77300E+01
1.32000E+02	5.96100E+01
1.52000E+02	8.40200E+01
1.72000E+02	1.34160E+02
1.85448E+02	1.95000E+02
3.50000E+02	1.95000E+02

Data for Fig.14 KJ and KIC for different flaws (a/w=0.05-0.9) and PTS transients

SB time=2100. sec.

a/w	KJ
5.00000E-02	4.36400E+01
1.00000E-01	5.47300E+01
1.50000E-01	6.21500E+01
2.00000E-01	6.74600E+01
2.50000E-01	7.17300E+01
3.00000E-01	7.41500E+01
4.00000E-01	7.97000E+01
5.00000E-01	8.42600E+01
6.00000E-01	8.79100E+01
7.00000E-01	9.09200E+01
8.00000E-01	9.18900E+01
9.00000E-01	9.04200E+01

RS time=2400. sec.

a/w	KJ
5.00000E-02	6.05800E+01
1.00000E-01	7.67300E+01
1.50000E-01	8.82100E+01
2.00000E-01	9.69300E+01
2.50000E-01	1.04340E+02
3.00000E-01	1.09040E+02
4.00000E-01	1.19890E+02
5.00000E-01	1.29420E+02
6.00000E-01	1.37700E+02
7.00000E-01	1.45370E+02
8.00000E-01	1.50470E+02
9.00000E-01	1.53630E+02

KIC: ART=170 C

a/w	KIC
5.00000E-02	6.53400E+01
1.00000E-01	7.36400E+01
1.50000E-01	8.36700E+01
2.00000E-01	9.56700E+01
2.50000E-01	1.09740E+02
3.00000E-01	1.26010E+02
4.00000E-01	1.64950E+02
5.00000E-01	1.95000E+02
6.00000E-01	1.95000E+02
7.00000E-01	1.95000E+02
8.00000E-01	1.95000E+02
9.00000E-01	1.95000E+02

KIC: ART=208 C

a/w	KIC
5.00000E-02	5.21900E+01
1.00000E-01	5.61800E+01
1.50000E-01	6.08000E+01
2.00000E-01	6.60700E+01
2.50000E-01	7.19600E+01
3.00000E-01	7.84300E+01
4.00000E-01	9.27800E+01
5.00000E-01	1.08300E+02
6.00000E-01	1.23810E+02
7.00000E-01	1.38070E+02
8.00000E-01	1.49700E+02
9.00000E-01	1.57630E+02

Data for Fig.15 Distribution of KJ along crack front for a/w=0.1-0.9 under SB-LOCA

a/w=0.1

degree	KJ
0.00000E+00	4.76200E+01
6.76000E+00	4.60800E+01
1.36100E+01	4.91100E+01
1.36100E+01	3.83700E+01
2.06700E+01	4.42600E+01
2.93400E+01	4.56100E+01
3.80200E+01	4.78800E+01
4.66900E+01	4.99800E+01
5.53200E+01	5.17300E+01
6.40000E+01	5.30600E+01
7.26900E+01	5.39800E+01
8.14300E+01	5.45300E+01
9.00000E+01	5.47300E+01

a/w=0.2

degree	KJ
0.00000E+00	6.49900E+01
3.37000E+00	6.22700E+01
6.76000E+00	6.82900E+01
6.76000E+00	5.35500E+01
1.71000E+01	5.62500E+01
2.62200E+01	5.82100E+01
3.53300E+01	6.07800E+01

4.44500E+01	6.30100E+01
5.35500E+01	6.47700E+01
6.26500E+01	6.60300E+01
7.17500E+01	6.68400E+01
8.08800E+01	6.73000E+01
9.00000E+01	6.74600E+01

a/w=0.3

degree	KJ
0.00000E+00	7.81000E+01
2.25000E+00	7.46400E+01
4.50000E+00	8.42300E+01
4.50000E+00	6.47600E+01
1.47700E+01	6.61900E+01
2.41700E+01	6.73900E+01
3.35800E+01	6.95800E+01
4.29800E+01	7.13700E+01
5.23900E+01	7.26400E+01
6.17800E+01	7.34400E+01
7.12000E+01	7.38700E+01
8.05600E+01	7.40800E+01
9.00000E+01	7.41500E+01

a/w=0.4

degree	KJ
0.00000E+00	9.09300E+01
1.69000E+00	8.69300E+01
3.37000E+00	1.00190E+02
3.37000E+00	7.65200E+01
1.36100E+01	7.66700E+01
2.31600E+01	7.68200E+01
3.27000E+01	7.82900E+01
4.22600E+01	7.93000E+01
5.18000E+01	7.98100E+01
6.13600E+01	7.99400E+01
7.09100E+01	7.98600E+01
8.04600E+01	7.97500E+01
9.00000E+01	7.97000E+01

a/w=0.5

degree	KJ
0.00000E+00	1.03710E+02
1.35000E+00	9.93600E+01
2.70000E+00	1.16540E+02

2.70000E+00	8.89500E+01
1.36100E+01	8.73600E+01
2.31600E+01	8.63700E+01
3.27100E+01	8.67800E+01
4.22600E+01	8.67300E+01
5.18000E+01	8.62900E+01
6.13600E+01	8.56200E+01
7.09000E+01	8.49300E+01
8.04400E+01	8.44400E+01
9.00000E+01	8.42600E+01

a/w=0.6

degree	KJ
0.00000E+00	1.16980E+02
1.12000E+00	1.12530E+02
2.25000E+00	1.33700E+02
2.25000E+00	1.01930E+02
1.30300E+01	9.88600E+01
2.26500E+01	9.62500E+01
3.22700E+01	9.53800E+01
4.18900E+01	9.40700E+01
5.15100E+01	9.24600E+01
6.11400E+01	9.07600E+01
7.07500E+01	8.92800E+01
8.03900E+01	8.82600E+01
9.00000E+01	8.79100E+01

a/w=0.7

degree	KJ
0.00000E+00	1.33850E+02
9.60000E-01	1.29740E+02
1.93000E+00	1.46250E+02
1.93000E+00	1.18770E+02
2.01500E+01	1.07050E+02
2.88800E+01	1.04870E+02
3.76100E+01	1.02910E+02
4.63500E+01	1.00520E+02
5.50800E+01	9.78200E+01
6.38100E+01	9.51700E+01
7.25400E+01	9.29400E+01
8.12700E+01	9.14400E+01
9.00000E+01	9.09200E+01

a/w=0.8

degree	KJ
0.00000E+00	1.49980E+02
8.40000E-01	1.47060E+02
1.69000E+00	1.57650E+02
1.69000E+00	1.34550E+02
2.43200E+01	1.15770E+02
3.25300E+01	1.13630E+02
4.07400E+01	1.10470E+02
4.89500E+01	1.06530E+02
5.71600E+01	1.02360E+02
6.53600E+01	9.83700E+01
7.35800E+01	9.49900E+01
8.18000E+01	9.27000E+01
9.00000E+01	9.18900E+01

a/w=0.9

degree	KJ
0.00000E+00	1.68160E+02
7.50000E-01	1.67300E+02
1.50000E+00	1.68610E+02
1.50000E+00	1.51880E+02
2.80700E+01	1.24880E+02
3.58100E+01	1.21990E+02
4.35500E+01	1.17200E+02
5.13000E+01	1.11660E+02
5.90400E+01	1.05820E+02
6.67700E+01	1.00090E+02
7.45200E+01	9.51100E+01
8.22700E+01	9.16600E+01
9.00000E+01	9.04200E+01

Data for Fig.16 Distribution of KJ along crack front for a/w=0.1-0.9 under RS PTS

a/w=0.1

degree	KJ
0.00000E+00	6.58000E+01
6.76000E+00	6.38300E+01
1.36100E+01	6.81100E+01
1.36100E+01	5.31200E+01
2.06700E+01	6.12400E+01
2.93400E+01	6.32000E+01
3.80200E+01	6.65200E+01
4.66900E+01	6.96200E+01

5.53200E+01	7.22100E+01
6.40000E+01	7.42100E+01
7.26900E+01	7.56000E+01
8.14300E+01	7.64300E+01
9.00000E+01	7.67300E+01

a/w=0.2

degree	KJ
0.00000E+00	9.02600E+01
3.37000E+00	8.66200E+01
6.76000E+00	9.49800E+01
6.76000E+00	7.45100E+01
1.71000E+01	7.84100E+01
2.62200E+01	8.15900E+01
3.53300E+01	8.56900E+01
4.44500E+01	8.93100E+01
5.35500E+01	9.22400E+01
6.26500E+01	9.43900E+01
7.17500E+01	9.58200E+01
8.08800E+01	9.66500E+01
9.00000E+01	9.69300E+01

a/w=0.3

degree	KJ
0.00000E+00	1.08890E+02
2.25000E+00	1.04220E+02
4.50000E+00	1.17530E+02
4.50000E+00	9.05500E+01
1.47700E+01	9.29200E+01
2.41700E+01	9.54200E+01
3.35800E+01	9.93900E+01
4.29800E+01	1.02780E+02
5.23900E+01	1.05360E+02
6.17800E+01	1.07140E+02
7.12000E+01	1.08240E+02
8.05600E+01	1.08840E+02
9.00000E+01	1.09040E+02

a/w=0.4

degree	KJ
0.00000E+00	1.27480E+02
1.69000E+00	1.22050E+02
3.37000E+00	1.40530E+02
3.37000E+00	1.07750E+02

1.36100E+01	1.08580E+02
2.31600E+01	1.10060E+02
3.27000E+01	1.13440E+02
4.22600E+01	1.16120E+02
5.18000E+01	1.17960E+02
6.13600E+01	1.19030E+02
7.09100E+01	1.19570E+02
8.04600E+01	1.19810E+02
9.00000E+01	1.19890E+02

a/w=0.5

degree	KJ
0.00000E+00	1.46330E+02
1.35000E+00	1.40390E+02
2.70000E+00	1.64500E+02
2.70000E+00	1.26250E+02
1.36100E+01	1.24960E+02
2.31600E+01	1.25300E+02
3.27100E+01	1.27580E+02
4.22600E+01	1.29090E+02
5.18000E+01	1.29840E+02
6.13600E+01	1.29950E+02
7.09000E+01	1.29750E+02
8.04400E+01	1.29510E+02
9.00000E+01	1.29420E+02

a/w=0.6

degree	KJ
0.00000E+00	1.66210E+02
1.12000E+00	1.60140E+02
2.25000E+00	1.90060E+02
2.25000E+00	1.45890E+02
1.30300E+01	1.42770E+02
2.26500E+01	1.41250E+02
3.22700E+01	1.42100E+02
4.18900E+01	1.42120E+02
5.15100E+01	1.41410E+02
6.11400E+01	1.40220E+02
7.07500E+01	1.38970E+02
8.03900E+01	1.38040E+02
9.00000E+01	1.37700E+02

a/w=0.7

degree	KJ
--------	----

0.00000E+00	1.91420E+02
9.60000E-01	1.85840E+02
1.93000E+00	2.09620E+02
1.93000E+00	1.71970E+02
2.01500E+01	1.57350E+02
2.88800E+01	1.57460E+02
3.76100E+01	1.56760E+02
4.63500E+01	1.55130E+02
5.50800E+01	1.52720E+02
6.38100E+01	1.50040E+02
7.25400E+01	1.47630E+02
8.12700E+01	1.45970E+02
9.00000E+01	1.45370E+02

a/w=0.8

degree	KJ
0.00000E+00	2.15800E+02
8.40000E-01	2.11930E+02
1.69000E+00	2.27460E+02
1.69000E+00	1.96910E+02
2.43200E+01	1.72800E+02
3.25300E+01	1.73830E+02
4.07400E+01	1.71400E+02
4.89500E+01	1.67490E+02
5.71600E+01	1.62900E+02
6.53600E+01	1.58270E+02
7.35800E+01	1.54240E+02
8.18000E+01	1.51460E+02
9.00000E+01	1.50470E+02

a/w=0.9

degree	KJ
0.00000E+00	2.43650E+02
7.50000E-01	2.42770E+02
1.50000E+00	2.44980E+02
1.50000E+00	2.24710E+02
2.80700E+01	1.89200E+02
3.58100E+01	1.90030E+02
4.35500E+01	1.85250E+02
5.13000E+01	1.79050E+02
5.90400E+01	1.72190E+02
6.67700E+01	1.65300E+02
7.45200E+01	1.59270E+02
8.22700E+01	1.55120E+02

9.00000E+01	1.53630E+02
-------------	-------------

Data for Fig.17 Temperature distribution through the wall thickness under LB-LOCA

time=2. sec.

WALL THICKNESS	TEMPERATURE
0.00000E+00	2.76051E+02
1.00000E+00	2.80241E+02
2.00000E+00	2.83176E+02
3.00000E+00	2.85239E+02
4.00000E+00	2.86722E+02
4.00100E+00	2.86722E+02
7.94102E+00	2.88149E+02
1.18810E+01	2.88592E+02
1.78530E+01	2.88768E+02
2.38250E+01	2.88791E+02
3.28768E+01	2.88800E+02
4.19286E+01	2.88800E+02
5.56485E+01	2.88800E+02
6.93685E+01	2.88800E+02
9.01640E+01	2.88800E+02
1.10960E+02	2.88800E+02
1.42480E+02	2.88800E+02
1.74000E+02	2.88800E+02

time=4. sec.

WALL THICKNESS	TEMPERATURE
0.00000E+00	2.51743E+02
1.00000E+00	2.62331E+02
2.00000E+00	2.70306E+02
3.00000E+00	2.76330E+02
4.00000E+00	2.80955E+02
4.00100E+00	2.80955E+02
7.94102E+00	2.85894E+02
1.18810E+01	2.87761E+02
1.78530E+01	2.88606E+02
2.38250E+01	2.88750E+02
3.28768E+01	2.88797E+02
4.19286E+01	2.88798E+02
5.56485E+01	2.88800E+02
6.93685E+01	2.88800E+02
9.01640E+01	2.88800E+02
1.10960E+02	2.88800E+02

1.42480E+02	2.88800E+02
1.74000E+02	2.88800E+02

time=6. sec.

WALL THICKNESS	TEMPERATURE
0.00000E+00	2.07893E+02
1.00000E+00	2.29614E+02
2.00000E+00	2.46256E+02
3.00000E+00	2.59118E+02
4.00000E+00	2.69250E+02
4.00100E+00	2.69250E+02
7.94102E+00	2.80624E+02
1.18810E+01	2.85519E+02
1.78530E+01	2.88058E+02
2.38250E+01	2.88613E+02
3.28768E+01	2.88787E+02
4.19286E+01	2.88792E+02
5.56485E+01	2.88800E+02
6.93685E+01	2.88799E+02
9.01640E+01	2.88800E+02
1.10960E+02	2.88800E+02
1.42480E+02	2.88800E+02
1.74000E+02	2.88800E+02

time=8. sec.

WALL THICKNESS	TEMPERATURE
0.00000E+00	1.37707E+02
1.00000E+00	1.76720E+02
2.00000E+00	2.06919E+02
3.00000E+00	2.30509E+02
4.00000E+00	2.49293E+02
4.00100E+00	2.49293E+02
7.94102E+00	2.70792E+02
1.18810E+01	2.80926E+02
1.78530E+01	2.86744E+02
2.38250E+01	2.88252E+02
3.28768E+01	2.88750E+02
4.19286E+01	2.88779E+02
5.56485E+01	2.88800E+02
6.93685E+01	2.88799E+02
9.01640E+01	2.88800E+02
1.10960E+02	2.88800E+02
1.42480E+02	2.88800E+02
1.74000E+02	2.88800E+02

time=9. sec.

WALL THICKNESS	TEMPERATURE
0.00000E+00	8.77869E+01
1.00000E+00	1.40575E+02
2.00000E+00	1.80214E+02
3.00000E+00	2.11027E+02
4.00000E+00	2.35542E+02
4.00100E+00	2.35542E+02
7.94102E+00	2.63575E+02
1.18810E+01	2.77352E+02
1.78530E+01	2.85629E+02
2.38250E+01	2.87924E+02
3.28768E+01	2.88711E+02
4.19286E+01	2.88767E+02
5.56485E+01	2.88800E+02
6.93685E+01	2.88798E+02
9.01640E+01	2.88800E+02
1.10960E+02	2.88800E+02
1.42480E+02	2.88800E+02
1.74000E+02	2.88800E+02

Data for Fig.18 KJ time history under LB-LOCA for a/w=0.05 and 0.25

a/w=0.05

TIME	KJ
2.00000E+00	1.27200E+01
4.00000E+00	1.24400E+01
6.00000E+00	1.36400E+01
8.00000E+00	2.07700E+01
9.00000E+00	2.60300E+01

a/w=0.25

TIME	KJ
2.00000E+00	2.58000E+01
4.00000E+00	1.70100E+01
6.00000E+00	6.82000E+00
8.00000E+00	6.54000E+00
9.00000E+00	8.25000E+00

Data for Fig.19 Comparison of KJ between surface and sub-surface flaw under SB-LOCA

a/w=0.25 surface flaw

degree	KJ
5.40000E+00	5.96900E+01
1.50000E+01	6.20900E+01
2.43700E+01	6.35400E+01
3.37500E+01	6.60100E+01
4.31200E+01	6.80900E+01
5.25100E+01	6.96300E+01
6.18700E+01	7.06600E+01
7.12300E+01	7.12800E+01
8.06100E+01	7.16200E+01
9.00000E+01	7.17300E+01

a/w=0.05 surface flaw

degree	KJ
2.80700E+01	3.29500E+01
3.52000E+01	3.80200E+01
4.20200E+01	3.88000E+01
4.89500E+01	3.99500E+01
5.58000E+01	4.10400E+01
6.26500E+01	4.19700E+01
6.94700E+01	4.27100E+01
7.63500E+01	4.32000E+01
8.31900E+01	4.35000E+01
9.00000E+01	4.36400E+01

a/w=0.25 sub-surface flaw

degree	KJ
5.40000E+00	3.29300E+01
1.50000E+01	3.42000E+01
2.43700E+01	4.11800E+01
3.37500E+01	4.50400E+01
4.31200E+01	4.74500E+01
5.25100E+01	4.89600E+01
6.18700E+01	4.99000E+01
7.12300E+01	5.04500E+01
8.06100E+01	5.07400E+01
9.00000E+01	5.08400E+01

a/w=0.05 sub-surface flaw

degree	KJ
2.80700E+01	8.27000E+00
3.52000E+01	9.49000E+00
4.20200E+01	1.33000E+01

4.89500E+01	1.54700E+01
5.58000E+01	1.68800E+01
6.26500E+01	1.79400E+01
6.94700E+01	1.87800E+01
7.63500E+01	1.93800E+01
8.31900E+01	1.97700E+01
9.00000E+01	1.99400E+01

Data for Fig.20 Comparison of KJ between surface and sub-surface flaw under RS PTS

a/w=0.25 surface flaw

degree	KJ
5.40000E+00	8.33800E+01
1.50000E+01	8.69400E+01
2.43700E+01	8.95900E+01
3.37500E+01	9.37500E+01
4.31200E+01	9.73500E+01
5.25100E+01	1.00150E+02
6.18700E+01	1.02120E+02
7.12300E+01	1.03390E+02
8.06100E+01	1.04100E+02
9.00000E+01	1.04340E+02

a/w=0.05 surface flaw

degree	KJ
2.80700E+01	4.56800E+01
3.52000E+01	5.26500E+01
4.20200E+01	5.37300E+01
4.89500E+01	5.53500E+01
5.58000E+01	5.68800E+01
6.26500E+01	5.82100E+01
6.94700E+01	5.92500E+01
7.63500E+01	5.99600E+01
8.31900E+01	6.03800E+01
9.00000E+01	6.05800E+01

a/w=0.25 sub-surface flaw

degree	KJ
5.40000E+00	4.59800E+01
1.50000E+01	4.75100E+01
2.43700E+01	5.77500E+01
3.37500E+01	6.37600E+01
4.31200E+01	6.77500E+01

5.25100E+01	7.04300E+01
6.18700E+01	7.22300E+01
7.12300E+01	7.33700E+01
8.06100E+01	7.40000E+01
9.00000E+01	7.42100E+01

a/w=0.05 sub-surface flaw
degree

	KJ
2.80700E+01	1.18600E+01
3.52000E+01	1.29200E+01
4.20200E+01	1.81400E+01
4.89500E+01	2.11600E+01
5.58000E+01	2.31300E+01
6.26500E+01	2.46100E+01
6.94700E+01	2.57900E+01
7.63500E+01	2.66300E+01
8.31900E+01	2.71800E+01
9.00000E+01	2.74200E+01

Data for Fig.21 Comparison of KJ between elastic and plastic calculations for sub-surface flaw

a/w=0.05 SB EL

degree	KJ
2.80700E+01	8.27000E+00
3.52000E+01	9.49000E+00
4.20200E+01	1.33000E+01
4.89500E+01	1.54700E+01
5.58000E+01	1.68800E+01
6.26500E+01	1.79400E+01
6.94700E+01	1.87800E+01
7.63500E+01	1.93800E+01
8.31900E+01	1.97700E+01
9.00000E+01	1.99400E+01

a/w=0.05 RS EL

degree	KJ
2.80700E+01	1.18600E+01
3.52000E+01	1.29200E+01
4.20200E+01	1.81400E+01
4.89500E+01	2.11600E+01
5.58000E+01	2.31300E+01
6.26500E+01	2.46100E+01

6.94700E+01	2.57900E+01
7.63500E+01	2.66300E+01
8.31900E+01	2.71800E+01
9.00000E+01	2.74200E+01

a/w=0.25 SB EL

degree	KJ
5.40000E+00	3.29300E+01
1.50000E+01	3.42000E+01
2.43700E+01	4.11800E+01
3.37500E+01	4.50400E+01
4.31200E+01	4.74500E+01
5.25100E+01	4.89600E+01
6.18700E+01	4.99000E+01
7.12300E+01	5.04500E+01
8.06100E+01	5.07400E+01
9.00000E+01	5.08400E+01

a/w=0.25 RS EL

degree	KJ
5.40000E+00	4.59800E+01
1.50000E+01	4.75100E+01
2.43700E+01	5.77500E+01
3.37500E+01	6.37600E+01
4.31200E+01	6.77500E+01
5.25100E+01	7.04300E+01
6.18700E+01	7.22300E+01
7.12300E+01	7.33700E+01
8.06100E+01	7.40000E+01
9.00000E+01	7.42100E+01

a/w=0.05 SB PL

degree	KJ
2.80700E+01	9.87000E+00
3.52000E+01	1.23600E+01
4.20200E+01	1.66600E+01
4.89500E+01	1.90600E+01
5.58000E+01	2.06700E+01
6.26500E+01	2.19000E+01
6.94700E+01	2.28500E+01
7.63500E+01	2.35000E+01
8.31900E+01	2.39100E+01
9.00000E+01	2.40800E+01

a/w=0.05 RS PL

degree	KJ
2.80700E+01	1.56200E+01
3.52000E+01	1.89100E+01
4.20200E+01	2.44300E+01
4.89500E+01	2.76400E+01
5.58000E+01	2.98900E+01
6.26500E+01	3.16100E+01
6.94700E+01	3.29500E+01
7.63500E+01	3.38900E+01
8.31900E+01	3.44500E+01
9.00000E+01	3.46900E+01

a/w=0.25 SB PL

degree	KJ
5.40000E+00	4.33600E+01
1.50000E+01	4.53500E+01
2.43700E+01	5.05400E+01
3.37500E+01	5.38500E+01
4.31200E+01	5.61600E+01
5.25100E+01	5.77500E+01
6.18700E+01	5.88100E+01
7.12300E+01	5.94700E+01
8.06100E+01	5.98300E+01
9.00000E+01	5.99500E+01

a/w=0.25 RS PL

degree	KJ
5.40000E+00	6.41500E+01
1.50000E+01	6.73400E+01
2.43700E+01	7.36200E+01
3.37500E+01	7.81400E+01
4.31200E+01	8.16700E+01
5.25100E+01	8.42800E+01
6.18700E+01	8.61300E+01
7.12300E+01	8.73400E+01
8.06100E+01	8.80200E+01
9.00000E+01	8.82500E+01

国際単位系(SI)と換算表

表1 SI基本単位および補助単位

量	名称	記号
長 質 量	メートル	m
時 間	キログラム	kg
電 流	秒	s
熱力学温度	アンペア	A
物 質 量	ケルビン	K
光 度	モル	mol
平 面 角	カンデラ	cd
立 体 角	ラジアン	rad
	ステラジアン	sr

表3 固有の名称をもつSI組立単位

量	名称	記号	他のSI単位による表現
周 波 数	ヘルツ	Hz	s^{-1}
力	ニュートン	N	$m \cdot kg/s^2$
圧 力、応 力	パスカル	Pa	N/m^2
エネルギー、仕事、熱量	ジュール	J	$N \cdot m$
工 率、放 射 束	ワット	W	J/s
電 気 量、電 荷	クーロン	C	$A \cdot s$
電 位、電 壓、起 電 力	ボルト	V	W/A
静 電 容 量	ファラード	F	C/V
電 気 抵 抗	オーム	Ω	V/A
コンダクタンス	ジーメンス	S	A/V
磁 束	ウェーバ	Wb	$V \cdot s$
磁 束 密 度	テスラ	T	Wb/m^2
インダクタンス	ヘンリー	H	Wb/A
セルシウス 温 度	セルシウス度	°C	
光 照 度	ルーメン	lm	$cd \cdot sr$
放 射 能	ルクス	lx	lm/m^2
吸 收 線 量	ベクレル	Bq	s^{-1}
線 量 当 量	グレイ	Gy	J/kg
	シーベルト	Sv	J/kg

表2 SIと併用される単位

名 称	記 号
分、時、日	min, h, d
度、分、秒	°, ', "
リットル	l, L
トントン	t
電子ボルト	eV
原子質量単位	u

$$1 \text{ eV} = 1.60218 \times 10^{-19} \text{ J}$$

$$1 \text{ u} = 1.66054 \times 10^{-27} \text{ kg}$$

表5 SI接頭語

倍数	接頭語	記号
10^{18}	エクサ	E
10^{15}	ペタ	P
10^{12}	テラ	T
10^9	ギガ	G
10^6	メガ	M
10^3	キロ	k
10^2	ヘクト	h
10^1	デカ	da
10^{-1}	デシ	d
10^{-2}	センチ	c
10^{-3}	ミリ	m
10^{-6}	マイクロ	μ
10^{-9}	ナノ	n
10^{-12}	ピコ	p
10^{-15}	フェムト	f
10^{-18}	アト	a

(注)

- 表1～5は「国際単位系」第5版、国際度量衡局1985年刊行による。ただし、1eVおよび1uの値はCODATAの1986年推奨値によった。
- 表4には海里、ノット、アール、ヘクタールも含まれているが日常の単位なのでここでは省略した。
- barは、JISでは流体の圧力を表わす場合に限り表2のカテゴリーに分類されている。
- EC閣僚理事会指令ではbar、barnおよび「血圧の単位」mmHgを表2のカテゴリーに入れている。

換 算 表

圧 力	MPa(=10 bar)	kgf/cm ²	atm	mmHg(Torr)	lbf/in ² (psi)
1	0.101972	0.224809			
9.80665	1	2.20462			
4.44822	0.453592	1			
粘 度 1 Pa·s(N·s/m ²)	= 10 P(ボアズ)(g/(cm·s))				
動粘度 1 m ² /s	= 10 ⁴ St(ストークス)(cm ² /s)				
力					
1	0.0980665	0.101325	1.33322 × 10 ⁻⁴	6.89476 × 10 ⁻³	145.038
9.80665	0.0980665	0.101325	1.35951 × 10 ⁻³	7.03070 × 10 ⁻²	14.2233
4.44822	0.0453592	0.013323	1.31579 × 10 ⁻³	6.80460 × 10 ⁻²	14.6959
			1	51.7149	1.93368 × 10 ⁻²

エネ ル ギ ー・仕 事・熱 量	J(=10 ⁷ erg)	kgf·m	kW·h	cal(計量法)	Btu	ft · lbf	eV	1 cal = 4.18605 J(計量法)	
								1	= 4.184 J(熱化学)
	1	0.101972	2.77778 × 10 ⁻⁷	0.238889	9.47813 × 10 ⁻⁴	0.737562	6.24150 × 10 ¹⁸		= 4.1855 J(15 °C)
	9.80665	1	2.72407 × 10 ⁻⁶	2.34270	9.29487 × 10 ⁻³	7.23301	6.12082 × 10 ¹⁹		= 4.1868 J(国際蒸気表)
	3.6 × 10 ⁶	3.67098 × 10 ⁵	1	8.59999 × 10 ⁵	3412.13	2.65522 × 10 ⁴	2.24694 × 10 ²⁵		
	4.18605	0.426858	1.16279 × 10 ⁻⁶	1	3.96759 × 10 ⁻³	3.08747	2.61272 × 10 ¹⁹	仕事率 1 PS(仏馬力)	
	1055.06	107.586	2.93072 × 10 ⁻⁴	252.042	1	778.172	6.58515 × 10 ²¹	= 75 kgf·m/s	
	1.35582	0.138255	3.76616 × 10 ⁻⁷	0.323890	1.28506 × 10 ⁻³	1	8.46233 × 10 ¹⁸	= 735.499 W	
	1.60218 × 10 ⁻¹⁹	1.63377 × 10 ⁻²⁰	4.45050 × 10 ⁻²⁶	3.82743 × 10 ⁻²⁰	1.51857 × 10 ⁻²²	1.18171 × 10 ⁻¹⁹	1		

放 射 能	Bq	Ci	吸 収 線 量	Gy	rad	照 射 線 量		線 量 当 量	Sv	rem
						1	100			
	1	2.70270 × 10 ⁻¹¹		0.01	1	1	100		1	100
	3.7 × 10 ¹⁰	1				2.58 × 10 ⁻⁴	1		0.01	1

照 射 線 量	C/kg	R	線 量 当 量	
			1	3876

(86年12月26日現在)

FRACTURE MECHANICS ANALYSIS AND EVALUATION FOR THE RPV OF THE CHINESE QINSHAN 300MW NPP UNDER PTS